

Universal Cosmologies

Paul Marconnet and Dimitrios Tsimpis

*Institut de Physique des Deux Infinis de Lyon
Université de Lyon, UCBL, UMR 5822, CNRS/IN2P3
4 rue Enrico Fermi, 69622 Villeurbanne Cedex, France*

marconnp@gmail.com, tsimpis@ipnl.in2p3.fr

Abstract

Universal cosmologies are exact solutions of 10d type IIA supergravity containing a 4d Friedmann-Lemaître-Robertson-Walker factor, that can also be repackaged as solutions of 4d models, i.e. as 4d consistent truncations. We extend the dynamical system analysis of universal cosmologies, beyond the case of a single exponential potential. For an open universe (negative 3d spatial curvature), these models generally possess many desirable features: parametric control of e-folds, late-time acceleration from potentials with steep exponentials (i.e. in accordance with swampland bounds), small string-loop and α' -corrections, scale separation and/or absence of decompactification.

Contents

1	Introduction	2
2	Two-scalar model	4
2.1	Dynamical system	5
2.2	Critical points	6
2.3	Analytic solutions	10
3	Single exponential potential	11
3.1	One-field consistent truncation	14
3.2	Heteroclinic orbit: unique analytic solution	14
4	Two-exponential potential	17
4.1	Critical Points	19
4.2	Stability	22
5	Universal compactifications	27
5.1	Late-time physics	28
6	Multi-exponential potential	33
7	Conclusions	34

1 Introduction

Obtaining realistic four-dimensional (4d) cosmologies from higher-dimensional supergravities arising from the low-energy limit of superstring theory is an interesting open question. Although it has been known for some time that time-dependent compactifications can lead to solutions exhibiting cosmic acceleration [1], thereby evading the no-go theorem of [2–4],¹ it was believed until recently that whenever such models [7–13] exhibit transient acceleration, the number of e-folds can be at most order one [14, 15].

In [16] we studied time-dependent solutions of Type IIA 10d supergravity with a 4d Friedmann-Lemaître-Robertson-Walker (FLRW) factor, compactified on different classes of 6d manifolds:

¹See [5, 6] for an improved version of the no-go that comprises the case of time-dependent compactifications.

Calabi-Yau, Einstein, Einstein-Kähler. The cosmologies thereby obtained were called “universal”, in that they only depend on the general features of the compactification manifolds. In addition we established a cosmological consistent truncation of IIA supergravity to a 4d gravitational theory coupled to two scalar fields, i.e. a repackaging of the 10d equations of motion such that every FLRW solution of the 4d theory lifts to a solution of 10d IIA supergravity.

Our work found that cosmologies — with or without Big Bang singularities — featuring late-time acceleration, or rollercoaster [17] asymptotic behavior, are generic in flux compactifications of 10d supergravity. Moreover, we showed that solutions exhibiting transient acceleration with a parametric control of e-folds are not only possible, but are also generic. The crucial ingredient in achieving these features is provided by the negative 3d spatial curvature: all these solutions require an open universe, i.e. a FLRW cosmology with hyperbolic 3d spatial slices. Interestingly, an open universe has been argued to be a generic prediction of the string landscape [18]. The recent results of [19] provide an additional compelling motivation to consider open cosmologies.

Ref. [20] put this analysis in the general context of 4d effective models with an exponential potential, and discussed their realization in string theory. It was explained therein that the steepness of the exponential potentials typically coming from supergravity (therefore in asymptotic regions of string theory, and in accordance with the swampland bounds [21–28]), in conjunction with the negative 3d curvature, guarantee the existence of the attractor fixed point on the boundary of the acceleration region — responsible for the features of the solutions of [16] mentioned in the previous paragraph. Moreover, it was emphasized that all these solutions have vanishing cosmological horizon, and conjectured that this may be a generic feature of theories of quantum gravity (see also [13, 29]).

Cosmological models have attracted a renewed interest within string theory [30–49], not least because of recent data providing evidence for a dynamical dark energy [50, 51]. Although steep single exponential models appear to be excluded by current observations [52–54], their multi-field, multi-exponential, spatially curved extensions warrant further study. In the present paper, we extend the dynamical system analysis of the universal cosmologies of [16] beyond the case of a single exponential potential, with a particular focus on the late-time physical properties of these models.

Our analysis confirms the presence of several phenomenologically desirable features. In addition to the aforementioned properties already noted in [16], we find that both loop corrections in the string coupling (g_s -corrections) and higher-order derivative corrections (α' -corrections) are generally suppressed at late times. Moreover, several models exhibit scale separation at late times, i.e. the ratio of the effective radius of their internal space to the 4d Hubble length vanishes at late times. This guarantees that, in addition to being 10d supergravity solutions, these models are also bona fide 4d effective descriptions.

The question of scale separation in cosmological solutions was recently revisited in [49], where it was noted that cosmologies supported by the curvature of the internal compactification space do not exhibit late time scale separation. We show that models in which the 6d curvature contributes non-trivially to the 4d potential at late times — even if its contribution is not dominant — also fail to exhibit scale separation. Instead, these models show an absence of decompactification, i.e. the effective radius of the internal space scales as the 4d Hubble

length at late times. This generalizes the results of [49], which focused on curvature-dominated potentials, to the cases where the potential merely includes a curvature contribution, in line with the results of [39] for flat universe.

In Section 2 we introduce the general framework of our models, from the point of view of a 4d gravitational theory minimally coupled to two scalar fields. At this stage we remain agnostic as to the possible higher-dimensional origin of this theory, aiming to provide the most general analysis. We introduce the dynamical system description of the part of the phase space that is independent of the details of the potential of the theory, the possible critical points and corresponding analytic solutions.

In Section 3 we specialize to the case of a single exponential potential. We review the critical points and their stability properties. In Section 3.1 we recall that in this case there always exists a consistent sub-truncation to a single scalar field, resulting in a theory whose potential generally has a steeper exponential than the original theory before truncation. In Section 3.2 we give the full analytic form of a cosmological solution exhibiting eternal acceleration and no Big Bang singularity.

In Section 4 we move on to the case of a two-exponential potential. We employ a set of phase space variables — different from the ones typically used in dynamical system descriptions of multi-exponential systems — that offer a visual, intuitive description of motion in phase space. The latter now contains a two-dimensional sub-plane, which can be thought of as the space of exponents of the potential. Points in that plane correspond to an effective exponent, constrained to move on a certain straight line. Moreover, the effective exponent at the stable critical point is given by the shortest vector connecting the origin of the plane to the convex hull of the two exponents of the potential.

In Section 5, we apply the tools developed above to the universal-cosmology models of [16], with a particular focus on their late-time behavior. We find that, in all but one model, both higher-order g_s - and α' -corrections are suppressed at late times. Moreover, all but one model avoid decompactification at late times, and three of these additionally exhibit scale separation. Finally, in Section 6 we comment on the multi-exponential case. We conclude in Section 7 with a discussion of future directions.

2 Two-scalar model

Our starting point is the 4d Einstein action with two minimally-coupled scalar fields,

$$S_{4d} = \int d^4x \sqrt{-g} \left(\frac{1}{16\pi G} R - \frac{1}{2} g^{\mu\nu} \sum_{i=1}^2 \partial_\mu \varphi_i \partial_\nu \varphi_i - V(\varphi_1, \varphi_2) \right), \quad (2.1)$$

where G is the 4d Newton's constant. In Section 5 we will interpret $\varphi_{1,2}$ as originating from the dilaton and the warp factor in 10d supergravity, but for now we will remain agnostic as to the potential higher-dimensional embedding of the action (2.1).

We are interested in cosmological solutions of FLRW form,

$$ds^2 = -dt^2 + a(t)^2 \left(\frac{dr^2}{1 - kr^2} + r^2 d\Omega^2 \right); \quad a(t) > 0, \quad (2.2)$$

where $a(t)$ is the scale factor and $k = \pm 1, k = 0$ corresponds to a closed, open, flat 4d universe respectively. Assuming homogeneous scalar fields, the matter equations of motion read,

$$\ddot{\varphi}_i + 3H\dot{\varphi}_i + \partial_{\varphi_i} V(\varphi) = 0 ; \quad i = 1, 2 , \quad (2.3)$$

where $H := \frac{\dot{a}}{a}$ is the Hubble parameter, and a dot stands for derivative with respect to the cosmological time t . The gravitational equations of motion are given by the two Friedman equations,²

$$\begin{aligned} H^2 &= \frac{8\pi G}{3}\rho - \frac{k}{a^2} \\ \dot{H} &= -4\pi G \sum_{i=1}^2 \dot{\varphi}_i^2 + \frac{k}{a^2} , \end{aligned} \quad (2.4)$$

where the energy density and pressure are given by,

$$\rho = \frac{1}{2} \sum_{i=1}^2 \dot{\varphi}_i^2 + V(\varphi) ; \quad p = \frac{1}{2} \sum_{i=1}^2 \dot{\varphi}_i^2 - V(\varphi) . \quad (2.5)$$

Moreover, it can be seen that, together with Eqs. (2.3), the first Friedman equation implies the second one.

2.1 Dynamical system

In order to rewrite the equations of motion in the form of a dynamical system, let us define [55],

$$\gamma_i(\varphi) := -\partial_{\varphi_i} \ln V ; \quad i = 1, 2 , \quad (2.6)$$

which are not constant in general. Furthermore, we set $8\pi G = 1$ and define the variables,³

$$N := \ln a , \quad x_1 := \frac{\dot{\varphi}_1}{H\sqrt{6}} , \quad x_2 := \frac{\dot{\varphi}_2}{H\sqrt{6}} , \quad z := \frac{\sqrt{V}}{H\sqrt{3}} , \quad H \neq 0 , \quad V \geq 0 . \quad (2.7)$$

In the following it will be useful to introduce a two-component vector notation, such that $\vec{x} = (x_1, x_2)$, $\vec{\gamma} = (\gamma_1, \gamma_2)$, etc. We thus obtain the following system of equations,

$$\begin{aligned} \vec{x}' &= \sqrt{\frac{3}{2}} \vec{\gamma} z^2 + \vec{x} (2\vec{x}^2 - z^2 - 2) \\ z' &= z \left(-\sqrt{\frac{3}{2}} \vec{\gamma} \cdot \vec{x} + 2\vec{x}^2 - z^2 + 1 \right) , \end{aligned} \quad (2.8)$$

where a prime denotes derivative with respect to N , together with the constraint,

$$\vec{x}^2 + z^2 = 1 + \frac{k}{a^2} . \quad (2.9)$$

²All equations of motion are invariant under the rescaling $k \rightarrow a_0^2 k$, $a \rightarrow a_0 a$, for any constant $a_0 > 0$.

³A negative potential can also be accommodated, by defining $z = \frac{\sqrt{|V|}}{H\sqrt{3}}$, which results in flipping the sign of z^2 in (2.8),(2.9). This implies in particular that there can be no acceleration if the potential is negative, as can be seen by flipping the sign of z^2 in (2.10). For this reason we restrict to non-negative potentials.

Eq. (2.9) only needs to be imposed at some initial time, as it is consistently propagated by the remaining equations. Eqs. (2.8), supplemented by the constraint (2.9), are a rewriting of (2.3), (2.4) in terms of the new variables. However (2.8) is not an autonomous dynamical system in general, unless $\vec{\gamma}$ happens to be constant.

Even without knowledge of the dynamics of $\vec{\gamma}(\varphi)$, there are a few important conclusions that we can draw from this system. Firstly, from the definition of the variable z , it follows that expanding cosmologies correspond to trajectories with $z > 0$. Secondly, from (2.4), (2.7) we have,

$$\frac{\ddot{a}}{a} = H^2(z^2 - 2\vec{x}^2) , \quad (2.10)$$

from which we see that accelerating cosmologies correspond to trajectories inside the cone in (\vec{x}, z) -space given by,

$$\mathcal{A} = \{(\vec{x}, z) \in \mathbb{R}^3 \mid z^2 > 2\vec{x}^2\} . \quad (2.11)$$

Thirdly, it follows from (2.8) that,

$$\frac{1}{2}(\vec{x}^2 + z^2)' = (z^2 - 2\vec{x}^2)(1 - \vec{x}^2 - z^2) . \quad (2.12)$$

Therefore the unit sphere,

$$\mathcal{S} = \{(\vec{x}, z) \in \mathbb{R}^3 \mid \vec{x}^2 + z^2 = 1\} , \quad (2.13)$$

is an invariant surface. This means that trajectories in the (\vec{x}, z) -space that cross \mathcal{S} at one point, must be entirely contained in \mathcal{S} . Furthermore, trajectories that have one point in the interior (exterior) of \mathcal{S} , must lie entirely in the interior (exterior) of \mathcal{S} . It then follows from (2.9) that open (closed) FLRW cosmologies correspond to trajectories in the interior (exterior) of \mathcal{S} , while flat cosmologies correspond to trajectories on \mathcal{S} .

In the following we will restrict our attention to FLRW cosmologies with $k \leq 0$.⁴ We can then see that, as a consequence of (2.11), (2.12), trajectories inside (outside) the acceleration region \mathcal{A} always move towards increasing (decreasing) distance from the origin of the (\vec{x}, z) -space.

2.2 Critical points

Independently of the dynamics of $\vec{\gamma}(\varphi)$, critical points of the system must necessarily be critical points of (2.8), i.e. solutions of $\vec{x}' = 0 = z'$ for $\vec{\gamma} = \vec{\gamma}_*$, where the constant vector $\vec{\gamma}_*$ is the value of $\vec{\gamma}$ at the critical point. In addition, the solution must satisfy the constraint (2.9). This leads to the following list of potential critical points, also depicted in Figure 1:

- All points $P_{\mathcal{C}} \in \mathcal{C}$ of the unit circle at the equator,

$$\mathcal{C} := \{(\vec{x}, z) \in \mathbb{R}^3 \mid \vec{x} = \vec{n} \text{ and } z = 0\} , \quad (2.14)$$

where \vec{n} is a constant unit vector, $|\vec{n}| = 1$. Being on the unit sphere \mathcal{S} , they require $k = 0$. Moreover the condition $z = 0$ implies $V = 0$. These points correspond to *kinetic domination*.

⁴The reason for this restriction is that, for the systems we are examining here, there can be no stable critical points with $k > 0$ [20, 56]. In particular, closed FLRW universes cannot exhibit (semi-)eternal acceleration.

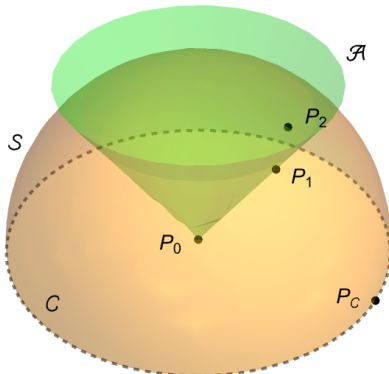


Figure 1: Critical points of the dynamical system, Eqs. (2.8), (2.9). The horizontal plane, vertical axis are parameterized by the coordinates \vec{x} , z respectively. The northern hemisphere of the unit surface \mathcal{S} is depicted — whose interior corresponds to expanding, open cosmologies. The green cone is the acceleration region \mathcal{A} . We depict a critical point P_C on the equator, i.e. the circle \mathcal{C} of kinetic energy dominated fixed points (dashed line); the curvature dominated critical point P_0 at the origin; the critical point P_2 with $\gamma^2 = 1.4$ on \mathcal{S} , and in the interior of \mathcal{A} ; the critical point P_1 with $\gamma^2 = 3.6$ on the boundary of \mathcal{A} , and in the interior of \mathcal{S} .

- The origin $P_0 = (0, 0, 0)$ of the (\vec{x}, z) -space. This point is in the interior of \mathcal{S} and has $z = 0$, it thus requires $k = -1$ and $V = 0$. In addition we must have $\dot{a}^2 = 1$ for the constraint to be satisfied, which implies vanishing acceleration. This point corresponds to *curvature domination*.
- The point $P_1 = (\vec{x}, z)$ with $z^2 = 2\vec{x}^2$ and $\vec{x} = \frac{\sqrt{2}}{\sqrt{3}\gamma_*^2} \vec{\gamma}_*$, where we have set $\gamma_* := |\vec{\gamma}_*|$. Being on the boundary of the acceleration cone \mathcal{A} , cf. (2.11), this point has vanishing acceleration. In addition we must have $\gamma_*^2 = 2 \left(1 + \frac{k}{\dot{a}^2}\right)^{-1}$ for the constraint (2.9) to be satisfied, which implies $\gamma_*^2 > 2$ for $k = -1$. This point corresponds to *curvature scaling*. It merges with P_0 , P_2 , for $\gamma_* \rightarrow \infty$, $\gamma_* \rightarrow \sqrt{2}$, respectively.
- The point $P_2 = (\vec{x}, z)$ with $z^2 = 1 - \vec{x}^2$ and $\vec{x} = \frac{1}{\sqrt{6}} \vec{\gamma}_*$, with $\gamma_*^2 < 6$. Being on the unit sphere \mathcal{S} , this point requires $k = 0$, and corresponds to *scalar domination*. It merges with P_C for $\gamma_* \rightarrow \sqrt{6}$. The limit $\gamma_* \rightarrow 0$, in which case P_2 merges with the north pole of \mathcal{S} , corresponds to constant potential and de Sitter universe.

Point	(\vec{x}, z)	Interpretation	Conditions
P_C	$(\vec{n}, 0)$	kinetic domination	$k = 0, V = 0$
P_0	$(0, 0, 0)$	curvature domination	$k = -1, V = 0$
P_1	$\frac{\sqrt{2}}{\sqrt{3}\gamma_*^2}(\vec{\gamma}_*, \sqrt{2}\gamma_*)$	curvature scaling	$k = -1, \gamma_*^2 > 2$
P_2	$\frac{1}{\sqrt{6}}(\vec{\gamma}_*, \sqrt{6 - \gamma_*^2})$	scalar domination	$k = 0, \gamma_*^2 < 6$

Table 1: Critical points of the dynamical system (2.8) subject to the constraint (2.9). We list their physical interpretation, their coordinates in the (\vec{x}, z) -space, and necessary existence conditions. The condition $V = 0$ for P_C, P_0 need only hold asymptotically. Additional existence conditions depend on the form of the potential. We have restricted to $z \geq 0$ and $k \leq 0$; $\vec{\gamma}_*$ is the value of $\vec{\gamma}$ at the critical point of the system, \vec{n} is an arbitrary unit vector, and $\gamma_* := |\vec{\gamma}_*|$.

The physical interpretation of the different fixed points can be seen from the analytic solutions of Section 2.3 below, and the corresponding energy balance between kinetic, potential, and curvature energy densities, $\Omega_{\text{kin}}, \Omega_{\text{pot}},$ and Ω_c respectively. More specifically, we define,

$$\rho_{\text{crit}} := \frac{3H^2}{8\pi G}; \quad \Omega_{\text{kin}} := \frac{\frac{1}{2}\dot{\vec{\varphi}}^2}{\rho_{\text{crit}}}; \quad \Omega_{\text{pot}} := \frac{V}{\rho_{\text{crit}}}; \quad \Omega_c := -\frac{k}{\dot{a}^2}, \quad (2.15)$$

so that,

$$\Omega_{\text{kin}} = \vec{x}^2; \quad \Omega_{\text{pot}} = z^2, \quad (2.16)$$

and (2.9) reads,

$$\Omega_{\text{kin}} + \Omega_{\text{pot}} + \Omega_c = 1. \quad (2.17)$$

The resulting energy budgets are displayed in Table 2.

Point	Ω_c	Ω_{kin}	Ω_{pot}
P_c	0	1	0
P_0	1	0	0
P_1	$1 - \frac{2}{\gamma_*^2}$	$\frac{2}{3\gamma_*^2}$	$\frac{4}{3\gamma_*^2}$
P_2	0	$\frac{\gamma_*^2}{6}$	$1 - \frac{\gamma_*^2}{6}$

Table 2: Energy budget at the fixed points. The critical points P_c , P_0 are fully dominated by the kinetic, curvature energy respectively. The energy budgets of P_1 and P_2 coincide for the limiting value $\gamma_* = \sqrt{2}$, for which the curvature energy density of P_1 vanishes.

The point P_1 will be of particular interest, as it is an attractor for potentials typically coming from low-energy effective models of string theory compactifications, i.e. with steep exponentials ($\gamma_*^2 > 2$) in accordance with the swampland conjectures [21–28]. In Fig. 2 we have plotted the dependence of the energy densities as a function of the effective exponent γ_* . The ratio of potential to kinetic energy at P_1 is γ_* -independent, $\Omega_{\text{pot}}/\Omega_{\text{kin}} = 2$.

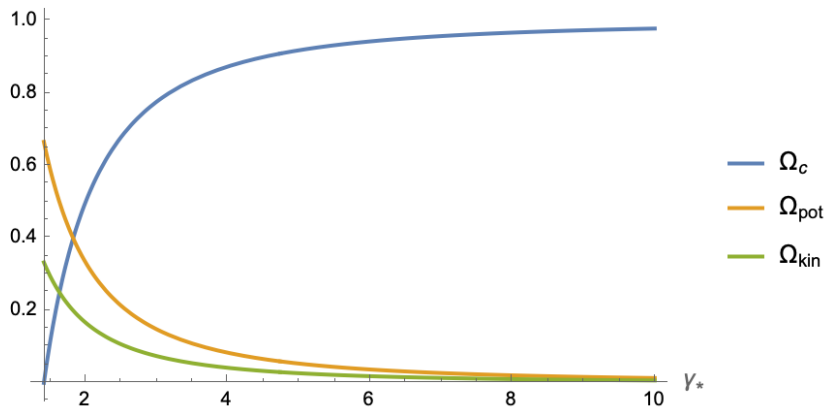


Figure 2: Curvature, potential and kinetic energy densities at the critical point P_1 , as functions of the effective exponent $\gamma_* \geq \sqrt{2}$. The curvature energy density vanishes for $\gamma_* \rightarrow \sqrt{2}$, while it completely dominates for $\gamma_* \rightarrow \infty$. The ratio $\Omega_{\text{pot}}/\Omega_{\text{kin}} = 2$ is γ_* -independent.

2.3 Analytic solutions

To obtain the explicit solutions at the critical points, we start by integrating (2.7), noting that $\frac{1}{H}\dot{\vec{\varphi}} = \vec{\varphi}'$, to obtain,

$$\vec{\varphi}_* = \vec{\varphi}_0 + \sqrt{6}\vec{x}_*N ; \quad \dot{\vec{\varphi}}_* = \sqrt{6}\vec{x}_*H , \quad (2.18)$$

for some constant vector $\vec{\varphi}_0$, where \vec{x}_* are the \vec{x} -coordinates of the critical point. For P_C , P_0 , for which $V = 0$, plugging the above into the equations of motion (2.3), (2.4) immediately leads to the analytic solution.

For the critical points P_1 , P_2 we proceed by evaluating (2.6) at the critical point to obtain,

$$V(\vec{\varphi}_*) = V_0 e^{-\vec{\gamma}_* \cdot \vec{\varphi}_*} , \quad (2.19)$$

for some constant $V_0 \geq 0$. Inserting this expression for V in the definition of z in (2.7) and integrating, then leads to,

$$a_*(t) = a_0 t^{\frac{\sqrt{2}}{\sqrt{3}\vec{\gamma}_* \cdot \vec{x}_*}} , \quad (2.20)$$

for some constant $a_0 > 0$, where we have used the time-translation invariance to set $a_*(0) = 0$. Plugging the above into the equations of motion (2.3), (2.4), then leads to certain additional algebraic conditions. The complete results of this analysis are summarized in Table 3. We see, in particular, that at each critical point,

$$\vec{\varphi}_*(t) = \vec{\varphi}_0 + c \vec{x}_* \ln t , \quad (2.21)$$

with c a proportionality factor that depends on the critical point.

Point	$a_*(t)$	$\vec{\varphi}_*(t)$	Conditions
P_C	$a_0 t^{\frac{1}{3}}$	$\vec{\varphi}_0 + \vec{n} \sqrt{\frac{2}{3}} \ln t$	$k = 0, V = 0$
P_0	t	$\vec{\varphi}_0$	$k = -1, V = 0$
P_1	$\frac{\gamma_*}{\sqrt{\gamma_*^2 - 2}} t$	$\vec{\varphi}_0 + \frac{2}{\gamma_*^2} \vec{\gamma}_* \ln t$	$k = -1$ $\vec{\gamma}_* \cdot \vec{\varphi}_0 = \ln \frac{\gamma_*^2 V_0}{4}$
P_2	$a_0 t^{\frac{2}{\gamma_*}}$	$\vec{\varphi}_0 + \frac{2}{\gamma_*^2} \vec{\gamma}_* \ln t$	$k = 0$ $\vec{\gamma}_* \cdot \vec{\varphi}_0 = \ln \frac{\gamma_*^4 V_0}{2(6 - \gamma_*^2)}$

Table 3: Explicit solution for $a(t)$ and $\vec{\varphi}(t)$ at the critical points of the dynamical system. The condition $V = 0$ for P_C , P_0 need only hold asymptotically. Additional existence conditions depend on the form of the potential. The quantities with a 0-subscript are free parameters, unless otherwise indicated. It is understood that $a_0 > 0$, and that \vec{n} is an arbitrary unit vector. We have used the time-translation invariance to set $a_*(0) = 0$.

Crucially, the question of stability, and any additional existence conditions of these critical points, depend on the dynamics of $\vec{\gamma}(\varphi)$, and thus on the exact form of V . In particular, additional existence conditions will generally be imposed by requiring that Eq. (2.19) be satisfied. Indeed, this equation is not automatic, unless V is a single exponential potential. We examine these questions in the following sections, in the context of (multi-)exponential potentials.

3 Single exponential potential

One scalar theories with a single exponential potential have been studied extensively, see [57] for the case of flat 3d space, and [58] for curved space with a barotropic fluid. Single exponential potentials with two fields and a barotropic fluid were discussed in [59] for flat space, while [60] also includes curvature and discusses the multi-field case.⁵

For a single exponential potential,

$$V(\varphi) = V_0 e^{-\vec{\gamma} \cdot \vec{\varphi}} ; \quad V_0 \geq 0 , \quad (3.1)$$

where $\vec{\gamma}$ and V_0 are constant, the dynamical system (2.8) is automatically autonomous, so no additional conditions arise for the existence of the critical points discussed in Section 2.2. In this case one can in fact use a field redefinition to decouple one of the two fields, and essentially reduce the theory to a single scalar with an exponential potential [56].⁶ We will come back to this point in Section 3.1.

The stability properties of the critical points are determined by studying the eigenvalues and corresponding eigenvectors of (2.8) at each critical point.

- At $P_{\mathcal{C}}$, the dynamical system has one positive eigenvalue (equal to 4) corresponding to a direction of approach along \vec{n} . It has one vanishing eigenvalue corresponding to the direction of approach in the \vec{x} -plane and perpendicular to \vec{n} , which is a reflexion of the fact that \mathcal{C} is a circle of fixed points. The third eigenvalue is equal to $\sqrt{\frac{3}{2}}(\sqrt{6} - \vec{\gamma} \cdot \vec{n})$, and corresponds to a direction of approach along $(0, 0, 1)$, i.e. a trajectory on \mathcal{S} approaching $P_{\mathcal{C}}$ along the z -direction. This eigenvalue is always positive for $\gamma^2 := |\vec{\gamma}|^2 < 6$. For $\gamma^2 > 6$ the sign depends on the angle between $\vec{\gamma}$ and \vec{n} . We can understand this as follows: for $\gamma^2 < 6$ the fixed point P_2 exists and it is an attractor for trajectories on \mathcal{S} (see below). In this case all trajectories on \mathcal{S} start at a point of \mathcal{C} end at P_2 . For $\gamma^2 > 6$ the point P_2 does not exist, and trajectories on \mathcal{S} starting at a point of \mathcal{C} end at another point of \mathcal{C} . I.e. in this case one segment of \mathcal{C}

⁵The case of a single exponential 4d potential corresponds, from the standpoint of the 1d consistent truncation of [16], to the “two-flux” case therein. Specifically, the system [16, Eq. (61)] reduces to (2.8) upon setting therein,

$$\begin{aligned} \alpha_1 &\rightarrow -\gamma_1 \sqrt{24} + 24 ; & \beta_1 &\rightarrow 6 ; & \gamma_1 &\rightarrow -\gamma_2 \frac{1}{\sqrt{2}} \\ \alpha_2 &\rightarrow 16 ; & \beta_2 &\rightarrow 4 ; & \gamma_2 &\rightarrow 0 , \end{aligned}$$

see also Section 5.

⁶This follows from the fact that (2.1),(3.1) are invariant under $\vec{\varphi} \rightarrow M \cdot \vec{\varphi}$, $\vec{\gamma} \rightarrow M \cdot \vec{\gamma}$, with $M \in O(2)$, which can be used to set e.g. $\gamma_2 = 0$ in the new basis, thus decoupling the corresponding scalar φ_2 .

consists of attractor points as concerns the approach along $(0, 0, 1)$, while the points of the complementary segment are repulsive.

- At $P_0 = (0, 0, 0)$, the dynamical system has one double negative eigenvalue (-2) corresponding to a direction of approach along the \vec{x} -plane. I.e. P_0 is an attractor for all trajectories in the \vec{x} -plane. Indeed all these trajectories start at some point of \mathcal{C} and end at P_0 . The third eigenvalue is positive $(+1)$ and corresponds to the unique trajectory (heteroclinic orbit) starting at P_0 and ending at P_1 .

- At P_1 we have one negative eigenvalue (-2) , corresponding to an approach parallel to the \vec{x} -plane and perpendicular to $\vec{\gamma}$. The remaining two eigenvalues are $-1 \pm \sqrt{8/\gamma^2 - 3}$, whose real part is always negative (recall that $\gamma^2 > 2$ for P_1 to exist). Moreover, if $\gamma > \gamma_s$, where,

$$\gamma_s := 2\sqrt{\frac{2}{3}}, \quad (3.2)$$

these eigenvalues are complex and P_1 is a stable spiral, while for $\gamma \leq \gamma_s$ the eigenvalues are real and P_1 is a stable node, see [20] for a recent discussion.

- At P_2 the system has one double eigenvalue given by $(\gamma^2 - 6)/2$, which is negative (recall that $\gamma^2 < 6$ for P_2 to exist), and corresponds to directions of approach tangent to the unit sphere \mathcal{S} . The third eigenvalue is given by $\gamma^2 - 2$ and can have either sign. For sufficiently flat exponential potential ($\gamma^2 < 2$), i.e. when P_1 does not exist, this eigenvalue is negative. In this case P_2 is the only fully stable critical point of the system. Conversely, for sufficiently steep exponential potential ($\gamma^2 > 2$), it is P_1 which is the only fully stable critical point.

The results of this analysis are summarized in Table 4. One important conclusion is that all open universes, which correspond to trajectories in the interior of the unit sphere \mathcal{S} , asymptote in the infinite past a fixed point $P_{\mathcal{C}}$ dominated by kinetic energy. For sufficiently steep exponential potential ($\gamma^2 > 2$) they asymptote the point P_1 in the future, otherwise (for $\gamma^2 < 2$) they asymptote P_2 , cf. Fig. 3.

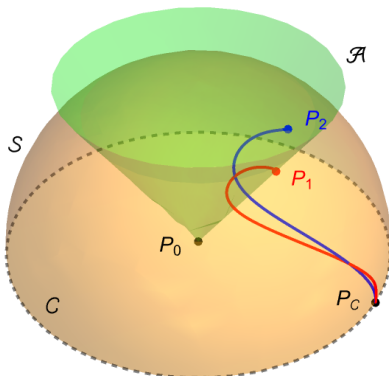


Figure 3: Two trajectories in the interior of the unit sphere \mathcal{S} , asymptoting at past infinity the point P_C on the equator \mathcal{C} . The blue trajectory asymptotes, at future infinity, the point P_2 with $\gamma^2 = 1.4$ on \mathcal{S} , and in the interior of the acceleration cone \mathcal{A} ; the red trajectory asymptotes the point P_1 with $\gamma^2 = 3.6$ on the boundary of \mathcal{A} , and in the interior of \mathcal{S} .

Point	(\vec{x}, z)	Eigenvalues	Conditions
P_C	$(\vec{n}, 0)$	$4, 0, \sqrt{\frac{3}{2}}(\sqrt{6} - \vec{\gamma} \cdot \vec{n})$	—
P_0	$(0, 0, 0)$	$-2, 1$	—
P_1	$\frac{\sqrt{2}}{\sqrt{3}\gamma^2}(\vec{\gamma}, \sqrt{2}\gamma)$	$-2, -1 \pm \frac{1}{\gamma}\sqrt{8 - 3\gamma^2}$	$\gamma^2 > 2$
P_2	$\frac{1}{\sqrt{6}}(\vec{\gamma}, \sqrt{6 - \gamma^2})$	$\frac{1}{2}(\gamma^2 - 6), \gamma^2 - 2$	$\gamma^2 < 6$

Table 4: Critical points of the single exponential potential: coordinates, eigenvalues and existence conditions for $\vec{\gamma}$. The point P_1 is fully stable whenever it exists (i.e. for $\gamma > \sqrt{2}$), while P_2 is fully stable whenever the complementary condition holds ($\gamma < \sqrt{2}$). The corresponding solutions at the critical points were given in Table 3. All trajectories in the interior of \mathcal{S} asymptote a point P_C at past infinity, and the fully stable point (P_1 or P_2) at future infinity.

Due to the fact that P_1 lies on the boundary of the acceleration cone \mathcal{A} , cosmologies that asymptote P_1 in the future always feature a period of accelerated expansion (which can be transient, eternal or semi-eternal). Moreover, as emphasized in [16, 20], the number of e-folds can be parametrically controlled, by adjusting the distance of the trajectory to the origin P_0 of the phase space, cf. [20, Figs. 7,8].

3.1 One-field consistent truncation

As already mentioned, for a single exponential potential one of the two scalar fields can be decoupled by a field redefinition. This can also be seen directly from the dynamical system: with $\vec{\gamma}$ being constant in the single exponential case, an additional consequence of (2.8) is that the plane,

$$\mathcal{P} := \{(\vec{x}, z) \in \mathbb{R}^3 \mid x_1\gamma_2 - x_2\gamma_1 = 0\} , \quad (3.3)$$

is an invariant surface. Indeed from (2.8) we have,

$$x'_1\gamma_2 - x'_2\gamma_1 = -[z^2 + 2(1 - x_1^2 - x_2^2)](x_1\gamma_2 - x_2\gamma_1) . \quad (3.4)$$

It follows from the above and the definition (2.7) of \vec{x} , that restricting to trajectories on \mathcal{P} is equivalent to setting $\varphi_1\gamma_2 - \varphi_2\gamma_1$ equal to an arbitrary constant, thereby consistently truncating out one of the two scalars. Assuming $\gamma_1 \neq 0$ without loss of generality, this consistent truncation is thus obtained by setting,

$$\varphi_2 = \frac{\gamma_2}{\gamma_1}\varphi_1 + \text{const.} ; \quad \varphi := \frac{\gamma}{\gamma_1}\varphi_1 , \quad (3.5)$$

where $\gamma := |\vec{\gamma}|$, upon which the theory (2.1) truncates to,

$$S_{4d} = \int d^4x \sqrt{g} \left(\frac{1}{16\pi G} R - \frac{1}{2} g^{\mu\nu} \partial_\mu \varphi \partial_\nu \varphi - \tilde{V}_0 e^{-\gamma\varphi} \right) , \quad (3.6)$$

for some constant $\tilde{V}_0 \geq 0$, in general different from V_0 of (3.1). In particular we see that the one-field truncation can only increase the effective exponent of the potential, since $|\vec{\gamma}| \geq |\gamma_1|, |\gamma_2|$.

The resulting model has a two-dimensional phase space, parameterized by z , as given in (2.7), and x defined by,

$$x := \frac{\dot{\varphi}}{H\sqrt{6}} , \quad (3.7)$$

so that (2.8), (2.9) remain valid, provided we simply replace \vec{x} by x .

3.2 Heteroclinic orbit: unique analytic solution

Pure higher-dimensional gravity compactified on Einstein manifolds was considered in [61]. In particular, the cosmological solutions of the 10d model compactified on a 6d hyperbolic space were shown to exhibit late-time acceleration. In [16] we pointed out that these models admit cosmological solutions with transient acceleration and parametric control of e-folds.

We will now show that the cosmological solution corresponding to the unique trajectory (called a *heteroclinic orbit* in dynamical system terminology) asymptoting the critical point P_0 in the past and the critical point P_1 in the future can be given analytically in the special case $\gamma = \gamma_s$, the threshold value above (below) which P_1 is a stable spiral (node), cf. Eq. (3.2). As was noted in [16], the critical point P_0 corresponds to a smooth 4d geometry (a Milne universe) that is reached at finite proper time in the past. The orbit can thus be geodesically completed

beyond P_0 to $t < 0$, using the time-reversal symmetry of Eqs. (2.3), (2.4): it corresponds to an eternally accelerating solution without Big Bang singularity.⁷

We first note that for general γ we can obtain the solution of the unique trajectory asymptotically in the neighborhood of the origin of phase space $x = z = 0$. Indeed, from (2.8), we obtain a perturbative expansion for x, z in terms of N ,

$$\begin{aligned} \frac{\sqrt{6}}{\gamma}x(N) &= \frac{3}{4}a^2 - \frac{1}{2^4}(10 + 3\gamma^2)a^4 + \frac{5}{2^{10}}(112 + 78\gamma^2 + 9\gamma^4)a^6 + \dots \\ z(N) &= a - \frac{1}{2^4}(8 + 3\gamma^2)a^3 + \frac{1}{2^9}(192 + 160\gamma^2 + 21\gamma^4)a^5 + \dots, \end{aligned} \quad (3.8)$$

where $a = e^N$, so that (x, z) tends to the origin of phase space (P_0) asymptotically in the past, $N \rightarrow -\infty$, $a \rightarrow 0$, in a direction of approach along the z -axis.⁸ These expansions can be straightforwardly obtained to any desired order in a .

As it turns out, in the special case $\gamma = \gamma_s$, from the series expansions (3.8) we can guess the closed expressions,

$$x = \frac{1}{2} \left(1 - \frac{1}{\sqrt{1 + 2a^2}} \right); \quad z = \frac{a}{\sqrt{1 + 2a^2}}, \quad (3.9)$$

which, as we verify a posteriori, correspond to bona fide solutions of the equations of motion (see below). Moreover, asymptotically in the future, $N, a \rightarrow \infty$, the solution tends to,

$$(x, z) = \left(\frac{1}{2}, \frac{1}{\sqrt{2}} \right), \quad (3.10)$$

which are indeed the coordinates of P_1 for the special case (3.2), cf. Table 4. I.e. although we obtained the solution by initially expanding around P_0 , the analytic solution (3.9) remains valid for the entire length of the orbit from P_0 to P_1 .

In order to obtain the analytic solution in terms of the original variables of the cosmological model, $\varphi(t)$, $a(t)$, we proceed as follows. Integrating (2.7), taking (3.9) into account, we find,

$$\varphi = \varphi_{-\infty} + \sqrt{\frac{3}{2}} \ln \left(\frac{1 + \sqrt{1 + 2a^2}}{2} \right), \quad (3.11)$$

where the constant $\varphi_{-\infty}$ is given by,

$$e^{2\sqrt{\frac{2}{3}}\varphi_{-\infty}} = \frac{1}{3}V_0, \quad (3.12)$$

so that for $N \rightarrow -\infty$, $a \rightarrow 0$, we have $\varphi \rightarrow \varphi_{-\infty}$. Moreover, integrating the constraint (2.9) we obtain,

$$t = \frac{1}{2}a + \frac{1}{2\sqrt{2}} \operatorname{arcsinh}(\sqrt{2}a), \quad (3.13)$$

⁷As pointed out in [16], in the vicinity of $t = 0$, the solution describes a de Sitter space in hyperbolic slicing,

$$ds^2 = -dt^2 + \sinh^2(t) \left(\frac{dr^2}{1+r^2} + r^2 d\Omega^2 \right).$$

Indeed, as it can be seen directly from Footnote 9, $a(t) = \sinh(t)$, up to and including $\mathcal{O}(t^3)$ terms.

⁸Explicitly, we substitute $x = \sum_{i=1}^{\infty} \varepsilon^i \delta x^{(i)}$, $z = \sum_{i=1}^{\infty} \varepsilon^i \delta z^{(i)}$ into (2.8), and we solve for $\delta x^{(i)}$, $\delta z^{(i)}$ order-by-order in ε . The approach along the z -axis is imposed by setting $\delta x^{(0)} = 0$. The auxiliary parameter ε may be set to one at the end.

where we have imposed, without loss of generality, that $t \rightarrow 0$ as $a \rightarrow 0$. Eq. (3.13) implicitly defines $a(t)$, and thus also $\varphi(t)$, via (3.11).⁹

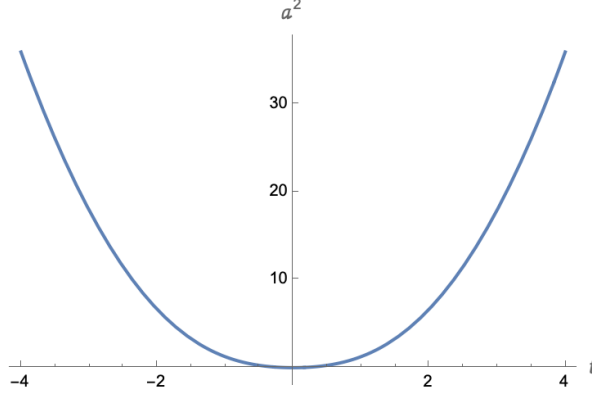


Figure 4: Plot of the scale factor of the heteroclinic orbit as a function of cosmological time. The cosmology is accelerating for all t ; it is expanding (contracting) for $t > 0$ ($t < 0$). The 4d geometry remains smooth at the apparent singularity $a = 0$, in the vicinity of which spacetime is quasi de Sitter.

We can directly verify that the analytic solution (3.11)-(3.13) satisfies the equations of motion (2.3), (2.4). To that end it suffices to use,

$$H = \frac{dN}{dt} = \frac{2\sqrt{1+2a^2}}{a(1+\sqrt{1+2a^2})}, \quad (3.14)$$

which follows from (3.13), in order to convert derivatives with respect to t to derivatives with respect to N . We can also verify that in the limit $t \rightarrow 0$ ($t \rightarrow \infty$), the solution (3.11)-(3.13) asymptotes the analytic solution at the critical point P_0 (P_1) given in Table 3.

The energy densities (2.15) along the heteroclinic orbit can also be given analytically,

$$\Omega_{\text{pot}} = \frac{a^2}{1+2a^2}; \quad \Omega_{\text{kin}} = \frac{(-1+\sqrt{1+2a^2})^2}{4(1+2a^2)}; \quad \Omega_c = \frac{(1+\sqrt{1+2a^2})^2}{4(1+2a^2)}. \quad (3.15)$$

In the asymptotic future (P_1) we have $\Omega_{\text{pot}} \rightarrow \frac{1}{2}$, and $\Omega_{\text{kin}}, \Omega_c \rightarrow \frac{1}{4}$. In the asymptotic past (P_0) we have $\Omega_c \rightarrow 1$, and $\Omega_{\text{kin}}, \Omega_{\text{pot}} \rightarrow 0$, in accordance with Table 2 for $\gamma_* = \gamma_s$.

⁹ The dilaton and the scale factor can be given explicitly as functions of cosmological time, for any γ , and to any desired order in a perturbative expansion around $t = 0$,

$$a = t + \frac{1}{6}t^3 + \frac{1}{15 \cdot 2^6}(8 - 27\gamma^2)t^5 + \mathcal{O}(t^7)$$

$$\frac{1}{\gamma}(\varphi - \varphi_{-\infty}) = \frac{3}{8}t^2 - \frac{1}{2^6}(2 + 3\gamma^2)t^4 + \frac{1}{15 \cdot 2^{11}}(112 + 342\gamma^2 + 225\gamma^4)t^6 + \mathcal{O}(t^8).$$

However we have been unable to find a closed expression for the right-hand sides of the equations above, even for the special case $\gamma = \gamma_s$.

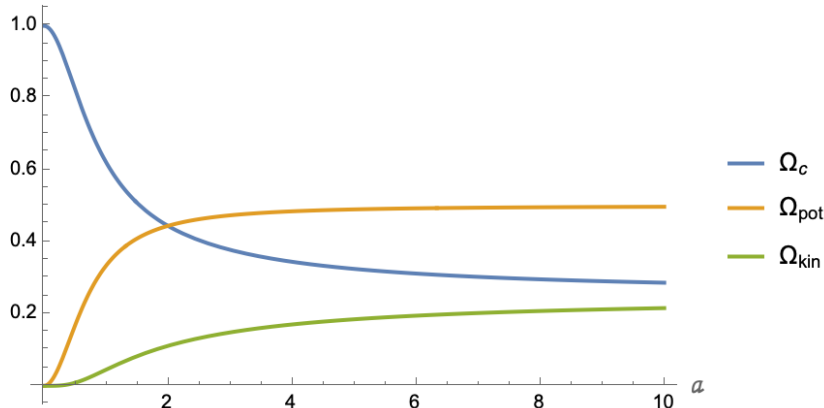


Figure 5: The evolution of the energy densities along the heteroclinic orbit from P_0 , in the past ($a \rightarrow 0$), to P_1 in the asymptotic future ($a \rightarrow \infty$). The energy densities at the endpoints of the orbit asymptote those for P_0, P_1 given in Table 2 for $\gamma_* = \gamma_s$.

4 Two-exponential potential

Let us now consider a two-exponential potential with “exponents” $\vec{\alpha}, \vec{\beta}$,

$$V(\varphi) = Ae^{-\vec{\alpha} \cdot \vec{\varphi}} + Be^{-\vec{\beta} \cdot \vec{\varphi}} , \quad (4.1)$$

where A, B , are real constants. We will assume $\vec{\alpha} \neq \vec{\beta}$, otherwise we are back to the single exponential potential case discussed in Section 3. For the reasons already mentioned in Footnote 3, we are interested in non-negative potentials, so we may assume $A \geq 0$ without loss of generality, while allowing B to have either sign.

Two-exponential potentials with one scalar field were discussed in [62–64]. Multi-exponential potentials with a different scalar field in each exponential were considered in [65, 66]. This is the setup of what is usually referred to as *assisted inflation*, and corresponds, in our notation, to having $\vec{\alpha} \cdot \vec{\beta} = 0$.¹⁰ The case of multi-exponential potentials with multiple fields in each exponential, called *generalized assisted inflation* in the literature, was discussed in [67, 68] for flat 3d space, while partial results concerning non-vanishing 3d curvature were given in [56].

The system (2.8),(2.9) now has to be supplemented with the dynamical equations for $\vec{\gamma}(\varphi)$,

$$\gamma'_i = \sum_{j=1}^2 \sqrt{6} x_j (\gamma_i \gamma_j - \gamma_{ij}) , \quad (4.2)$$

where we defined [55, 69],

$$\gamma_{ij}(\varphi) := \frac{\partial_{\varphi_i} \partial_{\varphi_j} V}{V} . \quad (4.3)$$

¹⁰To see this, use the invariance discussed in Footnote 6 so that in the new basis e.g. $\vec{\alpha} \propto (1, 0)$ and $\vec{\beta} \propto (0, 1)$.

For the potential (4.1), the parenthesis on right hand side of (4.2) is given in terms of the γ_i 's,

$$\gamma_i \gamma_j - \gamma_{ij} = (\alpha_i - \beta_i)(\alpha_j - \beta_j) \frac{(\alpha_1 \gamma_2 - \alpha_2 \gamma_1)(\beta_1 \gamma_2 - \beta_2 \gamma_1)}{(\alpha_1 \beta_2 - \alpha_2 \beta_1)^2}, \quad (4.4)$$

hence the system (2.8), (4.2) is autonomous. We may then rewrite (4.2),(4.4) as,

$$\vec{\gamma}' = \frac{\sqrt{6}(\vec{\alpha} \wedge \vec{\gamma}) \cdot (\vec{\beta} \wedge \vec{\gamma})}{|\vec{\alpha} \wedge \vec{\beta}|^2} [(\vec{\alpha} - \vec{\beta}) \cdot \vec{x}] (\vec{\alpha} - \vec{\beta}), \quad (4.5)$$

where the vector products among the two-component vectors $\vec{\alpha}, \vec{\beta}, \vec{\gamma}$ in (4.5) should be thought of as embedded in an auxiliary three-dimensional space. This is simply a calculational trick that allows us to rewrite (4.2) in vector notation.

The dynamical system (2.8), (4.5), subject to the constraint (2.9), is thus five-dimensional: cosmologies now correspond to trajectories in $(\vec{x}, z, \vec{\gamma})$ -space. These phase space variables are different from the so called ‘‘EN variables’’ [55] typically used in multi-exponential systems [70, 71]. Moreover, the projection of the motion onto the $\vec{\gamma}$ -plane admits a simple, intuitive description. Indeed, as follows from its definition and the form of the potential, $\vec{\gamma}$ is constrained to move on the line connecting $\vec{\alpha}$ and $\vec{\beta}$.¹¹

To see this, let us first consider the case $A, B > 0$. Without loss of generality we can absorb these two constants by shifting $\vec{\varphi}$ by a constant vector, so that,

$$\vec{\gamma} = \mu \vec{\alpha} + (1 - \mu) \vec{\beta}; \quad \mu := \frac{e^{-(\vec{\alpha} - \vec{\beta}) \cdot \vec{\varphi}}}{e^{-(\vec{\alpha} - \vec{\beta}) \cdot \vec{\varphi}} + 1} \in (0, 1), \quad (4.6)$$

therefore $\vec{\gamma}$ is constrained to move on the segment of the line between the two vectors $\vec{\alpha}, \vec{\beta}$, cf. the black arrow in Fig. 6a.

Let us now consider the case where A, B are not both positive: $A > 0, B < 0$. Proceeding as in the previous case, we may absorb these constants in the definition of $\vec{\varphi}$, to obtain,

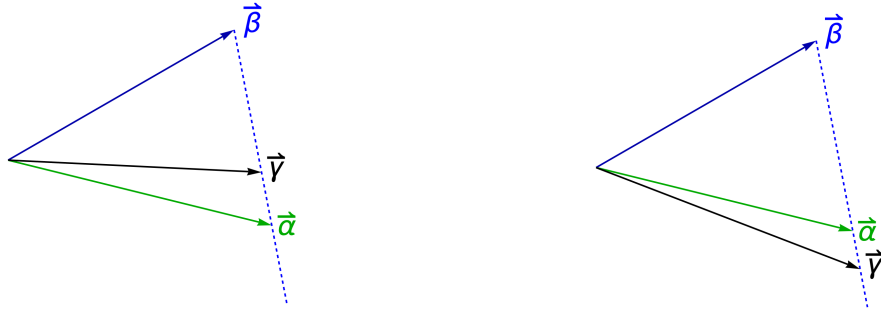
$$V = e^{-\vec{\beta} \cdot \vec{\varphi}} \left(e^{-(\vec{\alpha} - \vec{\beta}) \cdot \vec{\varphi}} - 1 \right). \quad (4.7)$$

The requirement that $V > 0$ thus constrains $e^{-(\vec{\alpha} - \vec{\beta}) \cdot \vec{\varphi}} \in (1, \infty)$, so that

$$\vec{\gamma} = \mu \vec{\alpha} + (1 - \mu) \vec{\beta}; \quad \mu := \frac{e^{-(\vec{\alpha} - \vec{\beta}) \cdot \vec{\varphi}}}{e^{-(\vec{\alpha} - \vec{\beta}) \cdot \vec{\varphi}} - 1} \in (1, \infty). \quad (4.8)$$

We see that $\vec{\gamma}$ is constrained to move on the exterior of the segment between the two vectors $\vec{\alpha}, \vec{\beta}$, and on the side of $\vec{\alpha}$, cf. the black arrow in Fig. 6b.

¹¹This is also consistent with (4.5), as can be seen from the fact that the right-hand side of that equation is proportional to $(\vec{\alpha} - \vec{\beta})$.



(a) The case $A, B > 0$: $\vec{\gamma}$ is constrained to lie on the segment between the two vectors $\vec{\alpha}, \vec{\beta}$.

(b) The case $A > 0, B < 0$: $\vec{\gamma}$ is constrained to lie on the exterior of the segment between the two vectors $\vec{\alpha}, \vec{\beta}$, and on the side of $\vec{\alpha}$.

Figure 6: Projection of motion onto the $\vec{\gamma}$ -plane. Restricting, without loss of generality, to the case $A > 0$, $\vec{\gamma}$ is constrained to lie on the semi-infinite line joining the two vectors $\vec{\alpha}, \vec{\beta}$, which starts at $\vec{\beta}$ and extends to the side of $\vec{\alpha}$ (dotted blue line).

The division of the line into three segments with boundaries given by $\vec{\alpha}, \vec{\beta}$, is consistent with the fact that $\vec{\gamma} = \vec{\alpha}, \vec{\beta}$ are critical points of the system (4.5). This ensures that $\vec{\gamma}$ can only reach the boundary of a segment asymptotically. In particular, $\vec{\gamma}$ cannot cross over to a segment that would violate the $V \geq 0$ condition.

4.1 Critical Points

The critical points of the five-dimensional system (2.8), (4.5), subject to the constraint (2.9), must now, in addition to the conditions discussed in Section 2.2, also satisfy $\vec{\gamma}' = 0$. In view of the right-hand side of (4.5), one way this condition is solved is if $\vec{\gamma}$ is parallel to $\vec{\alpha}$ or $\vec{\beta}$. Moreover, since $\vec{\gamma}$ is constrained to move on the line connecting $\vec{\alpha}$ and $\vec{\beta}$, this is equivalent to,

$$\vec{\gamma}_* = \vec{\alpha} \quad \text{or} \quad \vec{\gamma}_* = \vec{\beta}, \quad (4.9)$$

which means that the potential is dominated by one of the two exponentials. Therefore this case reduces to the one already discussed in Section 2.2, and no additional conditions arise, other than $A > 0$ (for the case $\vec{\gamma}_* = \vec{\alpha}$) or $B > 0$ (for the case $\vec{\gamma}_* = \vec{\beta}$), ensuring that the potential remains positive at the critical point.

The remaining possibility for the right-hand side of (4.5) to vanish, is that \vec{x} is perpendicular to $(\vec{\alpha} - \vec{\beta})$ at the critical point. This is equivalent to the condition that both exponentials scale in the same way at the critical point, as can be seen from (2.21),(4.1). In the following will therefore impose,

$$\vec{x}_* \cdot (\vec{\alpha} - \vec{\beta}) = 0. \quad (4.10)$$

Let us now examine the implications of (4.10) for each of the critical points of Table 1:

- At P_C we have $\vec{x}_* = \vec{n}$, and the condition (4.10) is not satisfied, in general, except for the two antipodal points of the equator for which \vec{n} is perpendicular to $(\vec{\alpha} - \vec{\beta})$ — in which case $\vec{\gamma}_*$ is unconstrained. This can also be seen directly from (2.19), which then reduces to,

$$\vec{n} \cdot \vec{\alpha} = \vec{n} \cdot \vec{\beta} = \vec{n} \cdot \vec{\gamma}_*, \quad (4.11)$$

which is simply the statement that $\vec{\gamma}_*$ can lie anywhere on the line connecting $\vec{\alpha}$ and $\vec{\beta}$.

- At P_0 the conditions (4.10), (2.19) are automatically satisfied, therefore $\vec{\gamma}_*$ is unconstrained.
- At P_1 the conditions (4.10), (2.19) reduce to,

$$\vec{\alpha} \cdot \vec{\gamma}_* = \vec{\beta} \cdot \vec{\gamma}_* = \gamma_*^2, \quad (4.12)$$

which can be solved to determine $\vec{\gamma}_*$ in terms of $\vec{\alpha}$, $\vec{\beta}$,¹²

$$\vec{\gamma}_* = \vec{\gamma}_\perp := \frac{(\vec{\alpha} - \vec{\beta}) \wedge (\vec{\beta} \wedge \vec{\alpha})}{|\vec{\alpha} - \vec{\beta}|^2}; \quad \gamma_* = |\vec{\gamma}_\perp| = \frac{|\vec{\alpha} \wedge \vec{\beta}|}{|\vec{\alpha} - \vec{\beta}|}. \quad (4.13)$$

This is the statement that $\vec{\gamma}_*$ is the height, $\vec{\gamma}_\perp$, of the triangle formed by $\vec{\alpha}$, $\vec{\beta}$, cf. Figure 7.



(a) The case $\theta_1, \theta_2 < \frac{\pi}{2}$: $\vec{\gamma}_* = \vec{\gamma}_\perp$ is stable; it is in the allowed range of $\vec{\gamma}$ iff $A, B > 0$.

(b) The case $\theta_1 > \frac{\pi}{2}, \theta_2 < \frac{\pi}{2}$: $\vec{\gamma}_* = \vec{\gamma}_\perp$ is unstable; it is in the allowed range of $\vec{\gamma}$ iff $A > 0, B < 0$.

Figure 7: $\vec{\gamma}_* = \vec{\gamma}_\perp$ at the critical points P_1, P_2 , as given in (4.13): it corresponds to the height of the triangle formed by $\vec{\alpha}, \vec{\beta}$; we are assuming $A > 0$, without loss of generality. The conditions (4.14), (4.15) are satisfied iff $\vec{\gamma}_\perp$ is within the allowed range of $\vec{\gamma}$, cf. Fig. 6.

Finally, inserting the solution for $a_*(t)$, $\vec{\varphi}_*(t)$ at P_1 from Table 3, with $\vec{\gamma}_*$ as given in (4.13), into the equations of motion (2.3), (2.4), we obtain two additional conditions,

$$\vec{\alpha} \cdot \vec{\varphi}_0 = \ln \left(\frac{A |\vec{\alpha} \wedge \vec{\beta}|^2}{4 \vec{\beta} \cdot (\vec{\beta} - \vec{\alpha})} \right); \quad \vec{\beta} \cdot \vec{\varphi}_0 = \ln \left(\frac{B |\vec{\alpha} \wedge \vec{\beta}|^2}{4 \vec{\alpha} \cdot (\vec{\alpha} - \vec{\beta})} \right). \quad (4.14)$$

It can readily be checked, taking (2.19), (4.13) into account, that these imply the condition $\vec{\gamma}_* \cdot \vec{\varphi}_0 = \ln \frac{\gamma_*^2 V_0}{4}$ from Table 3.

Eqs. (4.14) admit a solution, provided the arguments of the logarithms in the equations above are positive. Specifically, A, B must have the same sign as $\vec{\beta} \cdot (\vec{\beta} - \vec{\alpha})$, $\vec{\alpha} \cdot (\vec{\alpha} - \vec{\beta})$, respectively. The latter scalar products having positive (negative) sign is equivalent to the angle θ_2 , respectively θ_1 , of the base of the triangle formed by $\vec{\alpha}, \vec{\beta}$ being smaller (greater) than $\frac{\pi}{2}$, cf. Fig. 7.

For $A, B > 0$, the conditions (4.14) are thus equivalent to $\theta_1, \theta_2 < \frac{\pi}{2}$. Equivalently, the height of the triangle must lie inside the segment joining the two vectors $\vec{\alpha}, \vec{\beta}$, cf. Fig. 7a. On the other hand, this is precisely the allowed range of $\vec{\gamma}$ for $A, B > 0$, cf. Fig. 6.

¹²It can be checked that in the $\vec{\alpha} \rightarrow \vec{\beta}$ limit, (4.13) remains well-defined and reduces to $\vec{\gamma}_* = \vec{\alpha} = \vec{\beta}$.

For $A > 0, B < 0$, the angle θ_1 must be greater than $\frac{\pi}{2}$ for (4.14) to be satisfied. Equivalently, the height of the triangle must lie on the line joining the two vectors $\vec{\alpha}, \vec{\beta}$, at a point exterior to the segment between the two vectors, and on the side of the vector $\vec{\alpha}$, cf. Fig. 7b. Again this precisely coincides with the allowed range of $\vec{\gamma}$, cf. Fig. 6.

We conclude that, in every case, the conditions (4.14) admit a solution if and only if $\vec{\gamma}_\perp$ lies within the allowed range of $\vec{\gamma}$.

• At P_2 the same reasoning as in the case of P_1 leads to the exact same conditions for $\vec{\gamma}_*$, given in (4.13). Moreover, inserting the solution for $a_*(t), \vec{\varphi}_*(t)$ at P_2 from Table 3 into the equations of motion (2.3), (2.4), we obtain two additional conditions,

$$\vec{\alpha} \cdot \vec{\varphi}_0 = \ln \left(\frac{\gamma_*^4 A}{2(6 - \gamma_*^2)} \frac{|\vec{\alpha} - \vec{\beta}|^2}{\vec{\beta} \cdot (\vec{\beta} - \vec{\alpha})} \right) ; \quad \vec{\beta} \cdot \vec{\varphi}_0 = \ln \left(\frac{\gamma_*^4 B}{2(6 - \gamma_*^2)} \frac{|\vec{\alpha} - \vec{\beta}|^2}{\vec{\alpha} \cdot (\vec{\alpha} - \vec{\beta})} \right) . \quad (4.15)$$

It can be checked that these imply the condition $\vec{\gamma}_* \cdot \vec{\varphi}_0 = \ln \frac{\gamma_*^4 V_0}{2(6 - \gamma_*^2)}$ from Table 3.

Eqs. (4.15) admit a solution, provided the arguments of the logarithms in the equations above are positive. This leads to exactly the same conditions as discussed below (4.14), since $\gamma_*^2 < 6$, by the requirement of existence of P_2 . We thus conclude that the conditions (4.15) admit a solution if and only if $\vec{\gamma}_\perp$ lies within the allowed range of $\vec{\gamma}$.

The results of this analysis are summarized in Table 5.

Point	$a_*(t)$	$\vec{\varphi}_*(t)$	Conditions
P_C	$a_0 t^{\frac{1}{3}}$	$\vec{\varphi}_0 + \vec{n} \sqrt{\frac{2}{3}} \ln t$	$k = 0, V = 0$ $\vec{n} \cdot (\vec{\alpha} - \vec{\beta}) = 0$
P_0	t	$\vec{\varphi}_0$	$k = -1, V = 0$
P_1	$\frac{\gamma_*}{\sqrt{\gamma_*^2 - 2}} t$	$\vec{\varphi}_0 + \frac{2}{\gamma_*} \vec{\gamma}_* \ln t$	$k = -1, \vec{\gamma}_* = \vec{\gamma}_\perp$ $\vec{\alpha} \cdot \vec{\varphi}_0 = \ln \left(\frac{A \vec{\alpha} \wedge \vec{\beta} ^2}{4 \vec{\beta} \cdot (\vec{\beta} - \vec{\alpha})} \right)$ $\vec{\beta} \cdot \vec{\varphi}_0 = \ln \left(\frac{B \vec{\alpha} \wedge \vec{\beta} ^2}{4 \vec{\alpha} \cdot (\vec{\alpha} - \vec{\beta})} \right)$
P_2	$a_0 t^{\frac{2}{\gamma_*}}$	$\vec{\varphi}_0 + \frac{2}{\gamma_*} \vec{\gamma}_* \ln t$	$k = 0, \vec{\gamma}_* = \vec{\gamma}_\perp$ $\vec{\alpha} \cdot \vec{\varphi}_0 = \ln \left(\frac{\gamma_*^4 A}{2(6 - \gamma_*^2)} \frac{ \vec{\alpha} - \vec{\beta} ^2}{\vec{\beta} \cdot (\vec{\beta} - \vec{\alpha})} \right)$ $\vec{\beta} \cdot \vec{\varphi}_0 = \ln \left(\frac{\gamma_*^4 B}{2(6 - \gamma_*^2)} \frac{ \vec{\alpha} - \vec{\beta} ^2}{\vec{\alpha} \cdot (\vec{\alpha} - \vec{\beta})} \right)$

Table 5: The explicit solutions for $a(t)$ and $\vec{\varphi}(t)$ at the critical points, for the two-exponential potential (4.1) with $\vec{\alpha} \neq \vec{\gamma}_* \neq \vec{\beta}$. This is the case where both exponentials scale in the same way at the critical point, see main text for more details. For $\vec{\gamma}_* = \vec{\alpha}$ or $\vec{\gamma}_* = \vec{\beta}$ the potential is dominated by one of the two exponentials, and the solutions reduce to those of Table 3, provided we replace V_0 therein by A or B respectively. The condition $V = 0$ for P_C, P_0 need only hold asymptotically. The conditions for P_1, P_2 admit a solution if and only if $\vec{\gamma}_\perp$, cf. (4.13), lies within the allowed range for $\vec{\gamma}$, cf. Fig. 6.

4.2 Stability

The stability properties of the critical points for the two-exponential potential are determined by the eigenvalues and eigenvectors of the five-dimensional system (2.8), (4.5). Let us first examine the case $\vec{\alpha} \neq \vec{\gamma}_* \neq \vec{\beta}$.

- At P_C the eigenvalues and eigenvectors of the single exponential potential, cf. Table 4, setting $\vec{\gamma} \rightarrow \vec{\gamma}_*$ therein, carry over to the present case. Imposing $\vec{n} \cdot (\vec{\alpha} - \vec{\beta}) = 0$, cf. Table 5, there are no new eigenvalues that arise. Two new eigenvectors, representing motion purely in the $\vec{\gamma}$ -plane, are associated to the zero-eigenvalue.
- At P_0 the eigenvalues and eigenvectors of Table 4, also extend to the present case. In addition, there is a double zero-eigenvalue associated with eigenvectors purely in the $\vec{\gamma}$ -plane.
- At P_1 the eigenvalues $-1 \pm \frac{1}{\gamma_*} \sqrt{8 - 3\gamma_*^2}$ and the corresponding eigenvectors of Table 4, also extend here, with $\vec{\gamma}_* = \vec{\gamma}_\perp$, cf. Table 5. In addition there is a zero-eigenvalue with corresponding eigenvector whose projection on the $\vec{\gamma}$ -plane is perpendicular to $(\vec{\alpha} - \vec{\beta})$. This eigenvalue should be discarded as unphysical, as it corresponds to motion that would take us

outside the allowed range of $\vec{\gamma}$.

Moreover, there are two eigenvalues given by,

$$-1 \pm \frac{1}{\gamma_*} \sqrt{\gamma_*^2 - 4 \vec{\alpha} \cdot (\vec{\gamma}_* - \vec{\beta})}, \quad (4.16)$$

with corresponding eigenvectors whose projection on the $\vec{\gamma}$ -plane is parallel to $(\vec{\alpha} - \vec{\beta})$. These eigenvalues have negative real part if and only if $\vec{\alpha} \cdot (\vec{\gamma}_* - \vec{\beta}) > 0$, or equivalently $\vec{\beta} \cdot (\vec{\gamma}_* - \vec{\alpha}) > 0$, where we took (4.12) into account. This will be true if we are in the case depicted in Fig. 7a, therefore we also must require $A, B > 0$, otherwise $\vec{\gamma}_*$ is not within the allowed range of $\vec{\gamma}$. If instead $\vec{\alpha} \cdot (\vec{\gamma}_* - \vec{\beta}) < 0$, we are in the case of Fig. 7b, and one of the eigenvalues has positive real part. We conclude that P_1 , with $\vec{\gamma}_* = \vec{\gamma}_\perp$, is stable if and only if $\theta_1, \theta_2 < \frac{\pi}{2}$ and $A, B > 0$.

The eigenvectors corresponding to (4.16) read,¹³

$$\left(-1 \pm \frac{1}{\gamma_*} \sqrt{\gamma_*^2 - 4 \vec{\alpha} \cdot (\vec{\gamma}_* - \vec{\beta})}, 0, 0, -\sqrt{6} \vec{\alpha} \cdot (\vec{\gamma}_* - \vec{\beta}), 0 \right). \quad (4.17)$$

The eigenvalue -2 of the single exponential case is recovered in the $\vec{\alpha} \rightarrow \vec{\beta}$ limit, in which case we have $\vec{\gamma}_* = \vec{\alpha} = \vec{\beta}$, and the corresponding eigenvector reduces to the one of the single exponential potential.

- At P_2 the eigenvalues $\frac{1}{2}(\gamma_*^2 - 6)$, $(\gamma_*^2 - 2)$ and the corresponding eigenvectors of Table 4 also extend here, with $\vec{\gamma}_* = \vec{\gamma}_\perp$, cf. Table 5. In addition there is a zero-eigenvalue with corresponding eigenvector whose projection on the $\vec{\gamma}$ -plane is perpendicular to $(\vec{\alpha} - \vec{\beta})$, and should therefore be discarded as unphysical.

Moreover, there are two eigenvalues,

$$\frac{1}{4}(\gamma_*^2 - 6) \left(1 \pm \sqrt{1 + \frac{8(\vec{\alpha} \cdot \vec{\beta} - \gamma_*^2)}{6 - \gamma_*^2}} \right), \quad (4.18)$$

with corresponding eigenvectors whose motion in the $\vec{\gamma}$ -plane is parallel to $(\vec{\alpha} - \vec{\beta})$. The condition for the real part of both these eigenvalues to be negative is exactly as in the case discussed for P_1 . Therefore P_2 , with $\vec{\gamma}_* = \vec{\gamma}_\perp$, is stable if and only if $\gamma_*^2 < 2$ and $\theta_1, \theta_2 < \frac{\pi}{2}$ and $A, B > 0$.

We summarize the results of this analysis in Table 6.

¹³Without loss of generality, in order to simplify the expressions, we have used the $O(2)$ symmetry of the theory, cf. Footnote 6, to impose $(\vec{\alpha} - \vec{\beta}) \propto (1, 0)$ and, consequently, $\vec{\gamma}_\perp \propto (0, 1)$.

Point	Eigenvalues	Stability
P_C	$4, 0, \sqrt{\frac{3}{2}}(\sqrt{6} - \vec{\gamma}_* \cdot \vec{n})$	unstable
P_0	$-2, 1, 0$	unstable
P_1	$-2, -1 \pm \frac{1}{\gamma_*} \sqrt{8 - 3\gamma_*^2}, -1 \pm \frac{1}{\gamma_*} \sqrt{\gamma_*^2 - 4\vec{\alpha} \cdot (\vec{\gamma}_* - \vec{\beta})}$	stable iff $\gamma_*^2 > 2$, $\theta_1, \theta_2 < \frac{\pi}{2}$ & $A, B > 0$
P_2	$\frac{1}{2}(\gamma_*^2 - 6), \gamma_*^2 - 2, \frac{1}{4}(\gamma_*^2 - 6) \left(1 \pm \sqrt{1 + \frac{8(\vec{\alpha} \cdot \vec{\beta} - \gamma_*^2)}{6 - \gamma_*^2}} \right)$	stable iff $\gamma_*^2 < 2$, $\theta_1, \theta_2 < \frac{\pi}{2}$ & $A, B > 0$

Table 6: Eigenvalues and stability of the critical points of the double exponential potential, for $\vec{\alpha} \neq \vec{\gamma}_* \neq \vec{\beta}$. At the stable critical point (P_1 if $\gamma_*^2 > 2$, or P_2 if $\gamma_*^2 < 2$) the effective exponent $\vec{\gamma}_*$ is given by $\vec{\gamma}_\perp$, cf. (4.13) & Table 5, and we are in the case of Figure 7a.

Next, let us examine the case $\vec{\gamma}_* = \vec{\alpha}$; we must also impose $A \geq 0$, in order to ensure $V \geq 0$ at the critical point.

- At P_C , in addition to the eigenvalues and eigenvectors of the single exponential potential, cf. Table 4, setting $\vec{\gamma} \rightarrow \vec{\gamma}_* = \vec{\alpha}$ therein, we have one new eigenvalue,

$$\sqrt{6} \vec{n} \cdot (\vec{\alpha} - \vec{\beta}), \quad (4.19)$$

corresponding to motion purely in the $\vec{\gamma}$ -space. One additional eigenvector corresponding to the zero eigenvalue represents motion along $\vec{\alpha}$ and should be discarded as unphysical.

- At P_0 the eigenvectors and eigenvalues are the same as for the case $\vec{\alpha} \neq \vec{\gamma}_* \neq \vec{\beta}$ discussed previously.
- At P_1 , in addition to the eigenvalues and eigenvectors of the single exponential potential, there is an unphysical zero-eigenvalue, with corresponding eigenvector whose projection on the $\vec{\gamma}$ -plane is perpendicular to $(\vec{\alpha} - \vec{\beta})$. Moreover there is one new eigenvalue,

$$\frac{2\vec{\alpha} \cdot (\vec{\alpha} - \vec{\beta})}{|\vec{\alpha}|^2}, \quad (4.20)$$

with associated eigenvector corresponding to motion parallel to $(\vec{\alpha} - \vec{\beta})$ in the $\vec{\gamma}$ -plane. The eigenvalue (4.20) is positive if $\theta_1 < \frac{\pi}{2}$, and we are in the case of Fig. 8a. Otherwise, (4.20) is negative and we are in the case of Fig. 8b. We conclude that P_1 , with $\vec{\gamma}_* = \vec{\alpha}$, is stable if and only if $\theta_1 > \frac{\pi}{2}$. If in addition, $A > 0$, $B < 0$, then $\vec{\gamma}_\perp$ lies within the allowed range for $\vec{\gamma}$ and there can be solutions interpolating in $\vec{\gamma}$ -space from the unstable $\vec{\gamma}_* = \vec{\gamma}_\perp$, cf. Fig. 7b, to the stable $\vec{\gamma}_* = \vec{\alpha}$ cf. Fig. 8b. If on the other hand $A, B > 0$, then $\vec{\gamma}_\perp$ lies within the allowed range for $\vec{\gamma}$, provided $\theta_1 < \frac{\pi}{2}$. In this case there can be solutions interpolating in $\vec{\gamma}$ -space from

the unstable $\vec{\gamma}_* = \vec{\alpha}$, cf. Fig. 8a, to the stable $\vec{\gamma}_* = \vec{\gamma}_\perp$, cf. Fig. 7a. This discussion extends similarly to the critical points with $\vec{\gamma}_* = \vec{\beta}$. These results are depicted in Fig. 9.



(a) The case $\theta_1, \theta_2 < \frac{\pi}{2}$: $\vec{\gamma}_* = \vec{\alpha}$ is unstable; $\vec{\gamma}_\perp$ is in the allowed range of $\vec{\gamma}$ if $A, B > 0$.

(b) The case $\theta_1 > \frac{\pi}{2}, \theta_2 < \frac{\pi}{2}$: $\vec{\gamma}_* = \vec{\alpha}$ is stable; $\vec{\gamma}_\perp$ is in the allowed range of $\vec{\gamma}$ if $A > 0, B < 0$.

Figure 8: $\vec{\gamma}_* = \vec{\alpha}$ at the critical points P_1, P_2 ; we are assuming $A > 0$ without loss of generality.



(a) The case $\theta_1, \theta_2 < \frac{\pi}{2}$ & $A, B > 0$: $\vec{\gamma}$ interpolates from $\vec{\gamma}_* = \vec{\alpha}$ to $\vec{\gamma}_* = \vec{\gamma}_\perp$.

(b) The case $\theta_1 > \frac{\pi}{2}, \theta_2 < \frac{\pi}{2}$ & $A > 0, B < 0$: $\vec{\gamma}$ interpolates from $\vec{\gamma}_* = \vec{\gamma}_\perp$ to $\vec{\gamma}_* = \vec{\alpha}$.



(c) The case $\theta_1, \theta_2 < \frac{\pi}{2}$ & $A, B > 0$: $\vec{\gamma}$ interpolates from $\vec{\gamma}_* = \vec{\beta}$ to $\vec{\gamma}_* = \vec{\gamma}_\perp$.

(d) The case $\theta_1 > \frac{\pi}{2}, \theta_2 < \frac{\pi}{2}$ & $A, B > 0$: $\vec{\gamma}$ interpolates from $\vec{\gamma}_* = \vec{\beta}$ to $\vec{\gamma}_* = \vec{\alpha}$.

Figure 9: Interpolating flows in $\vec{\gamma}$ -space, depicted with solid red lines, from an unstable to a stable $\vec{\gamma}_*$; we are assuming $A > 0$ without loss of generality.

- At P_2 , in addition to the eigenvalues and eigenvectors of the single exponential potential, there is one new eigenvalue,

$$\vec{\alpha} \cdot (\vec{\alpha} - \vec{\beta}), \quad (4.21)$$

with associated eigenvector corresponding to motion parallel to $(\vec{\alpha} - \vec{\beta})$ in the $\vec{\gamma}$ -plane. In

addition there is an unphysical zero-eigenvalue, with eigenvector whose projection on the $\vec{\gamma}$ -plane is perpendicular to $(\vec{\alpha} - \vec{\beta})$. The eigenvalue (4.21) is positive if and only if $\theta_1 < \frac{\pi}{2}$.

We summarize the results of this analysis in Table 7.

Point	Eigenvalues	Stability
P_C	$4, 0, \sqrt{\frac{3}{2}}(\sqrt{6} - \vec{\alpha} \cdot \vec{n}), \sqrt{6} \vec{n} \cdot (\vec{\alpha} - \vec{\beta})$	unstable
P_0	$-2, 1, 0$	unstable
P_1	$-2, -1 \pm \frac{1}{ \vec{\alpha} } \sqrt{8 - 3 \vec{\alpha} ^2}, \frac{2}{ \vec{\alpha} ^2} \vec{\alpha} \cdot (\vec{\alpha} - \vec{\beta})$	stable iff $ \vec{\alpha} ^2 > 2$, $\theta_1 > \frac{\pi}{2}, \theta_2 < \frac{\pi}{2}$ & $A > 0$
P_2	$\frac{1}{2}(\vec{\alpha} ^2 - 6), \vec{\alpha} ^2 - 2, \vec{\alpha} \cdot (\vec{\alpha} - \vec{\beta})$	stable iff $ \vec{\alpha} ^2 < 2$, $\theta_1 > \frac{\pi}{2}, \theta_2 < \frac{\pi}{2}$ & $A > 0$

Table 7: Eigenvalues and stability of the critical points of the double-exponential potential, for $\vec{\gamma}_* = \vec{\alpha}$ and $A \geq 0$. At the stable critical point (P_1 if $|\vec{\alpha}|^2 > 2$, or P_2 if $|\vec{\alpha}|^2 < 2$) we are in the case of Figure 8b. A similar analysis can be performed for $\vec{\gamma}_* = \vec{\beta}$, in which case we must have $B \geq 0$.

In all cases, at the fully stable critical point (P_1 if $\gamma_*^2 > 2$ or P_2 if $\gamma_*^2 < 2$), γ_* is equal to the distance of the origin of $\vec{\gamma}$ -space to the *convex hull* of the exponents $\vec{\alpha}, \vec{\beta}$, the interval depicted in black in Fig. 10. I.e. let $\vec{\gamma}_{ch}$ be the shortest vector connecting the origin of $\vec{\gamma}$ -space to the convex hull of $\vec{\alpha}, \vec{\beta}$; at the fully stable critical point we have,

$$\vec{\gamma}_* = \vec{\gamma}_{ch} . \quad (4.22)$$

Conversely, if $\vec{\gamma}_{ch}$ lies outside the allowed range of $\vec{\gamma}$, then $P_{1,2}$ are unstable.

Since here we are only dealing with two exponentials, introducing the notion of the convex hull is somewhat redundant: it is simply the base of the triangle formed by the two vectors $\vec{\alpha}, \vec{\beta}$. However, it becomes useful in the context of multi-exponential potentials, see e.g. [39]. Note that the distance of the origin to the convex hull of $\vec{\alpha}, \vec{\beta}$ is not always the same as the distance to the line defined by $\vec{\alpha}, \vec{\beta}$. Indeed, $\gamma_* = |\vec{\gamma}_\perp|$ in the case of Fig. 10a, whereas $\gamma_* > |\vec{\gamma}_\perp|$ in the case of Fig. 10b.



(a) The case $\theta_1, \theta_2 < \frac{\pi}{2}$ & $A, B > 0$: $\vec{\gamma}_* = \vec{\gamma}_\perp$. (b) The case $\theta_1 > \frac{\pi}{2}, \theta_2 < \frac{\pi}{2}$ & $A > 0$: $\vec{\gamma}_* = \vec{\alpha}$.

Figure 10: $\vec{\gamma}_*$, depicted in $\vec{\gamma}$ -space, at the stable critical point P_1 ($\gamma_*^2 > 2$), or P_2 ($\gamma_*^2 < 2$); we are assuming $A > 0$ without loss of generality. In all cases, $\vec{\gamma}_* = \vec{\gamma}_{ch}$, where $\vec{\gamma}_{ch}$ is the shortest vector connecting the origin to the convex hull of $\vec{\alpha}$, $\vec{\beta}$ (solid black line). Conversely, $P_{1,2}$ are unstable if $\vec{\gamma}_{ch}$ lies outside the allowed range of $\vec{\gamma}$.

5 Universal compactifications

In [16] we established a cosmological consistent truncation of IIA supergravity to a 4d gravitational theory coupled to two scalar fields of the form (2.1), originating from the 10d dilaton and the warp factor of the metric. The term ‘‘cosmological consistent truncation’’ means a repackaging of the 10d equations of motion, such that every FLRW solution of the 4d theory lifts to a solution of 10d IIA supergravity.¹⁴ Explicitly, the 4d potential is given by,¹⁵

$$V = \begin{cases} 36b_0^2 e^{-\sqrt{6}\varphi_1 - \sqrt{2}\varphi_2} + \frac{3}{4}c_0^2 e^{-\frac{7\varphi_1}{\sqrt{6}} + \frac{\varphi_2}{\sqrt{2}}} & \text{CY internal 3- and 4-form fluxes} \\ \frac{1}{4}c_\varphi^2 e^{-3\sqrt{\frac{3}{2}}\varphi_1 - \frac{\varphi_2}{\sqrt{2}}} + \frac{1}{4}m^2 e^{-\sqrt{\frac{3}{2}}\varphi_1 + \frac{5\varphi_2}{\sqrt{2}}} - 3\lambda e^{-2\sqrt{\frac{2}{3}}\varphi_1} & \text{E external 4-form flux} \\ \frac{3}{4}c_0^2 e^{-\frac{7\varphi_1}{\sqrt{6}} + \frac{\varphi_2}{\sqrt{2}}} + \frac{1}{4}m^2 e^{-\sqrt{\frac{3}{2}}\varphi_1 + \frac{5\varphi_2}{\sqrt{2}}} - 3\lambda e^{-2\sqrt{\frac{2}{3}}\varphi_1} & \text{EK internal 4-form flux} \\ \frac{1}{4}c_\varphi^2 e^{-3\sqrt{\frac{3}{2}}\varphi_1 - \frac{\varphi_2}{\sqrt{2}}} + \frac{3}{4}c_f^2 e^{-\frac{5\varphi_1}{\sqrt{6}} + \frac{3\varphi_2}{\sqrt{2}}} - 3\lambda e^{-2\sqrt{\frac{2}{3}}\varphi_1} & \text{EK internal 2-form, external 4-form} \end{cases} \quad (5.1)$$

where E, EK, or CY stands for a 6d compactification manifold of Einstein, Einstein-Kähler, or Calabi-Yau type. Depending on the class of the compactification manifold, and in order to preserve the consistency of the 4d truncation, only certain types of fluxes can be simultaneously turned on in the 10d theory. The remnant of these 10d fluxes is manifested in the potential of the 4d theory in the presence of certain constants, listed below in Table 8. These are precisely the constants of proportionality between the 10d fluxes and the universal forms of

¹⁴All solutions presented in [16] can be thought of as solutions of an appropriate 1d consistent truncation, of the kind used in minisuperspace. However, not all of the solutions of [16] admit a 4d consistent truncation. This is reflected in the fact that the potential of the 1d truncation, given in [16, Eq. (15)], is much richer than the 4d one, given here in (5.1).

¹⁵Unlike in [16], we have canonically normalized the scalar fields. Comparison of (2.1) of the present paper with the action of [16, Eq. (22)] gives, $A^{\text{there}} = \sqrt{\frac{\pi G}{3}} \varphi_1$, $\phi^{\text{there}} = \sqrt{16\pi G} \varphi_2$, $V^{\text{there}} = 16\pi G V$.

the compactification (volume, Kähler form, etc), and will in general be subject to quantization in the full-fledged quantum theory.

m	zero-form (Romans mass)
c_f	internal two-form
b_0	internal three-form
c_φ	external four-form
c_0	internal four-form
λ	scalar curvature of M_6

Table 8: List of the constant coefficients appearing in the potential (5.1) of the 4d consistent truncation, and their 10d origin. A form is called external (internal), if all its legs are along the 4d external (6d internal) directions.

Two-exponential models, with potential as in (4.1), can be formed by selecting two species of flux from within each class of compactification — corresponding to each of the four lines on the right-hand side of (5.1) — and reading off the corresponding constants A, B and exponents $\vec{\alpha}, \vec{\beta}$. The resulting models are listed in Table 9. At least one of A, B is always positive, since the only potentially negative coefficient in the potential (5.1) is -3λ , coming from compactification on a 6d Einstein space with scalar curvature λ . According to our convention we will always take $A > 0$, and so we will set $B = -3\lambda$ in all models coming from compactification on 6d Einstein spaces. This choice allows for B both positive or negative, corresponding to negative or positive 6d curvature respectively. For all models the allowed range of $\vec{\gamma}$ is as in Fig. 6.

For all the models in Table 9, we have $\gamma_*^2 > 2$, in accordance with the swampland conjectures [21–28]. This implies that the fully stable critical point is always P_1 , requiring an open universe. For the models with a 6d curvature contribution, i.e. those with $B = -3\lambda$, we must require $\lambda < 0$ for $\vec{\gamma}_{ch}$ to lie in the allowed range for $\vec{\gamma}$, so that P_1 is stable.

The smallest value for the effective exponent at the critical point is attained for the model from compactification on an Einstein space with negative curvature and non-vanishing Romans mass. For this model we have $\gamma_*^2 = \frac{50}{19}$, which is smaller than the threshold value, Eq. (3.2), below which P_1 is a stable node [20]. To our knowledge, this is the smallest effective exponent so far obtained from a universal compactification model.

Five of the models of Table 9 correspond to the case depicted in Fig. 7a. The remaining three models have $\vec{\gamma} = \vec{\beta}$ at the critical point, corresponding to the case depicted in Fig. 8b, with $(A, \vec{\alpha}, \theta_1)$ and $(B, \vec{\beta}, \theta_2)$ interchanged. In these models $\vec{\gamma}_\perp$ is always outside the allowed range for $\vec{\gamma}$, so there are no possible interpolating flows of the type depicted in Fig. 9b.

5.1 Late-time physics

As can be seen from [16, Eqs. (1),(4)] and Footnote 15, setting $8\pi G = 1$, the uplift of the universal cosmologies to the 10d Einstein frame is given by,

$$ds_{10}^2 = e^{-\sqrt{\frac{3}{2}}\varphi_1} ds^2 + e^{\frac{1}{\sqrt{6}}\varphi_1} ds^2(M_6) ; \quad e^\phi = e^{\sqrt{2}\varphi_2} , \quad (5.2)$$

where ϕ is the 10d dilaton, ds^2 is the FLRW metric (2.2) in the 4d Einstein frame, and $ds^2(M_6)$ is the time-independent metric of the internal compactification manifold M_6 .

In all cases, the late-time asymptotics ($t \rightarrow \infty$) are dictated by the attractor point P_1 , and the associated solution, cf. Table 5. This implies that at late times the solution behaves as,

$$a(t) = \frac{\gamma_*}{\sqrt{\gamma_*^2 - 2}} t + \mathcal{O}(t^{-1}) ; \quad \vec{\varphi} = \vec{\varphi}_0 + \frac{2}{\gamma_*^2} \vec{\gamma}_* \ln t + \mathcal{O}(t^{-1}) . \quad (5.3)$$

In particular, we will be interested in the late-time behavior of the string coupling and the Hubble length,

$$g_s := e^\phi , \quad L_H := \frac{1}{H} , \quad (5.4)$$

as well as the effective size of the compactification manifold. The latter is defined as the time-dependent Kaluza-Klein (KK) scale of M_6 , as measured in the 4d Einstein frame; it can be read off of the 10d metric (5.2),

$$L_6(t) := L_6 e^{\sqrt{\frac{2}{3}} \varphi_1} , \quad (5.5)$$

where L_6 is the KK scale of M_6 in the absence of a warp factor, see [49] for a recent discussion. Taking Eqs. (5.2), (5.3) into account, we thus have,

$$g_s \rightarrow e^{\sqrt{2}(\vec{\varphi}_0)_2} t^{2\sqrt{2} \frac{(\vec{\gamma}_*)_2}{\gamma_*^2}} ; \quad L_H \rightarrow t ; \quad L_6(t) \rightarrow L_6 e^{\sqrt{\frac{2}{3}}(\vec{\varphi}_0)_1} t^{2\sqrt{\frac{2}{3}} \frac{(\vec{\gamma}_*)_1}{\gamma_*^2}} , \quad (5.6)$$

in the $t \rightarrow \infty$ limit.

We will now briefly review the derivation of Eq. (5.5), in a way that will also allow us to obtain an estimate of higher-order derivative α' -corrections. For our purposes it is sufficient to consider the following 10d effective action,

$$S_{10} = \int d^{10}x \sqrt{-g_{10}} \sum_{n=0}^{\infty} (\alpha')^n (R_{10})^{n+1} , \quad (5.7)$$

where R_{10} , g_{10} is the scalar curvature, the determinant of the metric (5.2), respectively. Ignoring derivatives of φ_1 , we can rewrite the above as,

$$S_{10} = \int d^4x \sqrt{-g_4} \int d^6x \sqrt{g_6} \sum_{n=0}^{\infty} \left(\alpha' e^{\sqrt{\frac{3}{2}} \varphi_1} \right)^n \left(R_4 + e^{-2\sqrt{\frac{2}{3}} \varphi_1} R_6 \right)^{n+1} , \quad (5.8)$$

where g_6 , R_6 is the determinant, scalar curvature of $ds^2(M_6)$; g_4 , R_4 is the determinant, scalar curvature of ds^2 , cf. Eq. (5.2). From this, and the fact that R_6 scales as $1/L_6^2$, we can see that, from the point of view of the 4d Einstein frame, the 6d effective scale is given by $L_6(t)$ of Eq. (5.5). In addition, we see that for the α' -corrections to be small, we must have,

$$\alpha' e^{\sqrt{\frac{3}{2}} \varphi_1} R_4 \ll 1 \quad \& \quad \alpha' e^{-\frac{1}{\sqrt{6}} \varphi_1} R_6 \ll 1 . \quad (5.9)$$

Given that R_6 scales as $1/L_6^2$, while R_4 scales as $1/L_H^2$ [49], we arrive at the condition,

$$\text{Small } \alpha'\text{-corrections} \quad \Leftrightarrow \quad \frac{L_H}{L_6(t)} e^{\frac{1}{2\sqrt{6}} \varphi_1} \gg \frac{l_s}{L_6} \quad \& \quad e^{\frac{1}{2\sqrt{6}} \varphi_1} \gg \frac{l_s}{L_6} , \quad (5.10)$$

where $l_s := \sqrt{\alpha'}$ is the string length. In the absence of warp factor ($\varphi_1 = 0$), the last inequality reduces to the condition that the size of the compactification space should be large in string units — which is the usual necessary condition for the validity of the supergravity description of time-independent solutions.

Furthermore, let us define the *absence of decompactification*, as the condition that the effective KK length of the internal space should be at most of the order of the Hubble length,

$$\text{Absence of decompactification} \quad \Leftrightarrow \quad \frac{L_H}{L_6(t)} \gtrsim 1. \quad (5.11)$$

This condition prevents the internal space from expanding at a faster rate than the 4d space-time, but allows for backgrounds for which the two scales are of the same order, analogous to AdS vacua of Freund-Rubin type. Moreover it follows that,

$$\text{Absence of decompactification} \quad \& \quad e^{\frac{1}{2\sqrt{6}}\varphi_1} \gg \frac{l_s}{L_6} \quad \Rightarrow \quad \text{Small } \alpha'\text{-corrections} \quad (5.12)$$

Absence of decompactification is weaker than the condition of *scale separation*, which is usually defined as the condition that the radius of curvature of the 4d space should be much greater than the KK length of the internal space — a necessary condition for the 10d theory to admit a 4d low-energy effective description. Adapting this definition to the case of our time-dependent backgrounds, we have,

$$\text{Scale separation} \quad \Leftrightarrow \quad \frac{L_H}{L_6(t)} \gg 1. \quad (5.13)$$

For time-independent supergravity backgrounds originating from string/M-theory, the condition of scale separation is notoriously difficult to satisfy with only classical ingredients, in the absence of orientifolds [72–89].¹⁶ However, as was noted in [20, 39], and recently emphasized in [49], the situation is different for cosmological backgrounds. Besides the first model of Table 9, for which higher-order corrections blow up at late times and the internal space decompactifies, we distinguish the following cases.

Models with scale separation: the three models with $\gamma_*^2 = 8$. They all have the same effective exponent $\vec{\gamma}_* = \vec{\gamma}_\perp$, due to the fact that the potential in these models consists of exponential terms — those generated by the fluxes c_f, c_φ, m, c_0 — whose exponents all lie on the same line, cf. Table 9.

Models with curvature domination: the three models with $\vec{\gamma}_* = \vec{\beta} = (2\sqrt{\frac{2}{3}}, 0)$, whose potential is dominated at future infinity by the exponential associated with the internal curvature λ . These have $g_s \rightarrow \text{cnst}$, $L_6(t) \rightarrow t$ asymptotically, so they all exhibit absence of decompactification but no time-evolution driven scale separation. More precisely, the asymptotic behavior near the future attractor P_1 can be read off of Table 3 and Eq. (5.6),

$$g_s \rightarrow e^{\sqrt{2}(\vec{\varphi}_0)_2} ; \quad \frac{L_6(t)}{L_H} \rightarrow L_6 \sqrt{2|\lambda|}. \quad (5.14)$$

Moreover, the $(\vec{\varphi}_0)_2$ component remains undetermined asymptotically, so that g_s is a modulus, within the supergravity approximation, and can be tuned to be as small as desired.

¹⁶It was recently shown that scale separation is possible within the 6d Salam-Sezgin model [90].

On the other hand, the ratio $L_6(t)/L_H$ cannot be tuned by scaling the time-independent overall length L_6 of M_6 , since the scalar curvature λ itself scales as $1/L_6^2$. It might be possible, however, to obtain some degree of *relative* (as opposed to *parametric*) scale separation by modding out M_6 by discrete subgroups of its isometry group, as in [82, 91].

Model with curvature contribution: fourth model of Table 9. Its potential includes an exponential term proportional to λ , which contributes non-trivially asymptotically, but does not dominate (so that $\vec{\gamma}_* = \vec{\gamma}_\perp \neq \vec{\beta}$). In this case we have the exact same scaling for $L_6(t)$ asymptotically, as for the models with curvature domination. This follows from Eq. (5.6) and the fact that $(\vec{\gamma}_*)_1/\gamma_*^2 = 1/|\vec{\beta}|$. The latter has a simple geometric interpretation, cf. Fig. 11.

We conclude that models with asymptotically nontrivial curvature contribution, whether or not the latter dominates the potential, cannot achieve time-evolution driven scale separation. Instead, these models exhibit absence of decompactification, whereby the FLRW factor scales at late times in the same way as the internal space. This feature is independent of the ratio A/B . In other words, the asymptotic scaling of $L_6(t)$ is independent of the strength of the contribution of the curvature term to the potential, as long as this contribution is non-vanishing asymptotically. This generalizes the observations of [49] for curvature dominated potentials, to potentials with merely curvature contribution, in line with the results of [39] for flat universe.

On the other hand, the precise coefficient of the ratio of internal-to-external length depends on the exponents of the potential. For example, for the model at hand, this ratio can be calculated from Eq. (5.6), using the condition on $\vec{\varphi}_0$ from Table 5,

$$\frac{L_6(t)}{L_H} \rightarrow \frac{5}{2\sqrt{3}} L_6 \sqrt{|\lambda|}, \quad (5.15)$$

which is different from (5.14). In particular, the numerical coefficient of the ratio depends on the angle of $(\vec{\alpha}, \vec{\beta})$,

$$\frac{L_6(t)}{L_H} \rightarrow L_6 |\vec{\alpha} \wedge \vec{\beta}| \sqrt{\frac{3|\lambda|}{4\vec{\alpha} \cdot (\vec{\alpha} - \vec{\beta})}}, \quad (5.16)$$

and it tends to zero as this angle tends to π . It thus might be possible, by tuning this angle, to achieve an amount of relative scale separation, in models with curvature contribution.

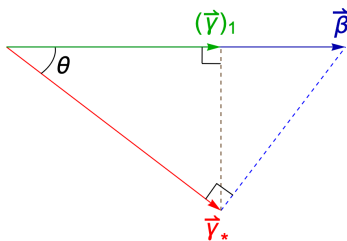


Figure 11: Model with 6d curvature term, in the case where the latter contributes but does not dominate asymptotically, i.e. $\vec{\gamma}_* = \vec{\gamma}_\perp \neq \vec{\beta}$. The relation $(\vec{\gamma}_*)_1/\gamma_* = \gamma_*/|\vec{\beta}| = \cos \theta$, ensures the same asymptotic scaling for $L_6(t)$, as in the case of curvature domination.

A	B	$\vec{\alpha}, \vec{\beta}, \vec{\gamma}_\perp$	$\vec{\gamma}_\perp$	$\vec{\gamma}_*$	γ_*^2	g_s	$e^{\sqrt{\frac{2}{3}}\varphi_1}$	$\frac{L_6(t)}{L_H}$	g_s, α'	Sc. S.
$\frac{3}{4}c_0^2$	$36b_0^2$		Y	$\vec{\gamma}_\perp$	$\frac{50}{7}$	$t^{\frac{1}{5}}$	$t^{\frac{3}{5}}$	$t^{\frac{2}{5}}$	N	N
$\frac{1}{4}c_\varphi^2$	$\frac{1}{4}m^2$		Y	$\vec{\gamma}_\perp$	8	$t^{-\frac{1}{2}}$	$t^{\frac{1}{2}}$	$t^{-\frac{1}{2}}$	Y	Y
$\frac{1}{4}c_\varphi^2$	-3λ		N	$\vec{\beta}$	$\frac{8}{3}$	t^0	t^1	t^0	Y	R
$\frac{1}{4}m^2$	-3λ		Y	$\vec{\gamma}_\perp$	$\frac{50}{19}$	$t^{-\frac{1}{5}}$	t^1	t^0	Y	R
$\frac{3}{4}c_0^2$	$\frac{1}{4}m^2$		Y	$\vec{\gamma}_\perp$	8	$t^{-\frac{1}{2}}$	$t^{\frac{1}{2}}$	$t^{-\frac{1}{2}}$	Y	Y
$\frac{3}{4}c_0^2$	-3λ		N	$\vec{\beta}$	$\frac{8}{3}$	t^0	t^1	t^0	Y	R
$\frac{1}{4}c_\varphi^2$	$\frac{3}{4}c_f^2$		Y	$\vec{\gamma}_\perp$	8	$t^{-\frac{1}{2}}$	$t^{\frac{1}{2}}$	$t^{-\frac{1}{2}}$	Y	Y
$\frac{3}{4}c_f^2$	-3λ		N	$\vec{\beta}$	$\frac{8}{3}$	t^0	t^1	t^0	Y	R

Table 9: Two-exponential models from universal compactifications. The constants A, B of each model are given in terms of the 10d fluxes, cf. Table 8. The vectors $\vec{\alpha}, \vec{\beta}, \vec{\gamma}_\perp$ are depicted in green, blue, red respectively. The column “ $\vec{\gamma}_\perp$ ” indicates whether or not (Y/N) the vector $\vec{\gamma}_\perp$ lies within the allowed range for $\vec{\gamma}$. For all models $A > 0$, and we are in the case of Fig. 6. The column “ $\vec{\gamma}_*$ ” indicates the value of $\vec{\gamma}$ at the stable critical point. For all models $\gamma_*^2 > 2$, and the stable critical point is P_1 . The models with 6d curvature must have $\lambda < 0$ for P_1 to be stable. The late time scalings of $g_s, \exp(\sqrt{\frac{2}{3}}\varphi_1), \frac{L_6(t)}{L_H}$ are listed in the respective columns. In the column “ g_s, α' ” we indicate whether or not these higher-order corrections can be tuned to be small at late times. The column “Sc. S.” indicates whether or not scale separation can be achieved at late times; “R” denotes the cases where relative scale separation might be possible.

6 Multi-exponential potential

Let us now briefly consider the case of a potential with n exponential terms, function of the two-component scalar $\vec{\varphi}$ as before,

$$V(\varphi) = \sum_{i=1}^n \Lambda_i e^{-\vec{\alpha}_i \cdot \vec{\varphi}} ; \quad V \geq 0 , \quad (6.1)$$

where some of the constants Λ_i may have negative signs. In the generic case, we expect the potential to be dominated near the stable critical point by at most two exponentials ($\vec{\alpha}_1, \vec{\alpha}_2$, for the example of Figure 12), and our previous results apply. We will therefore not enter into a detailed analysis here. More than two exponentials may contribute asymptotically in special cases where more than two exponents $\vec{\alpha}_i$ lie on the same line in $\vec{\gamma}$ -space.

Definition (2.6) now gives,

$$\vec{\gamma} = \frac{1}{V} \sum_{i=1}^n \vec{\alpha}_i \Lambda_i e^{-\vec{\alpha}_i \cdot \vec{\varphi}} . \quad (6.2)$$

The allowed region for $\vec{\gamma}$ can be determined with similar reasoning as in Section 4. We have depicted in Figure 12 the case of a three exponential potential ($n = 3$), with different possible signs for Λ_i . In the case $\Lambda_i > 0$ for $i = 1, 2, 3$, the allowed region for $\vec{\gamma}$ is the convex hull of the exponents $\vec{\alpha}_i$ — the shaded blue region of Figure 12,

$$\mu_1 \vec{\alpha}_1 + \mu_2 \vec{\alpha}_2 + (1 - \mu_1 - \mu_2) \vec{\alpha}_3 ; \quad \mu_1 + \mu_2 \leq 1 ; \quad \mu_1, \mu_2 \geq 0 . \quad (6.3)$$

The case $\Lambda_3 < 0, \Lambda_1, \Lambda_2 > 0$ is depicted in Figure 12a. The allowed region for $\vec{\gamma}$ in this case (shaded brown region) is given by,

$$\mu_1 \vec{\alpha}_1 + \mu_2 \vec{\alpha}_2 + (1 - \mu_1 - \mu_2) \vec{\alpha}_3 ; \quad \mu_1 + \mu_2 \geq 1 ; \quad \mu_1, \mu_2 \geq 0 . \quad (6.4)$$

Similarly, for $\Lambda_1 > 0, \Lambda_2, \Lambda_3 < 0$, the allowed region for $\vec{\gamma}$ is given by,

$$(1 - \mu_2 - \mu_3) \vec{\alpha}_1 + \mu_2 \vec{\alpha}_2 + \mu_3 \vec{\alpha}_3 ; \quad \mu_2, \mu_3 \leq 0 , \quad (6.5)$$

which corresponds to the brown shaded region of Figure 12b.

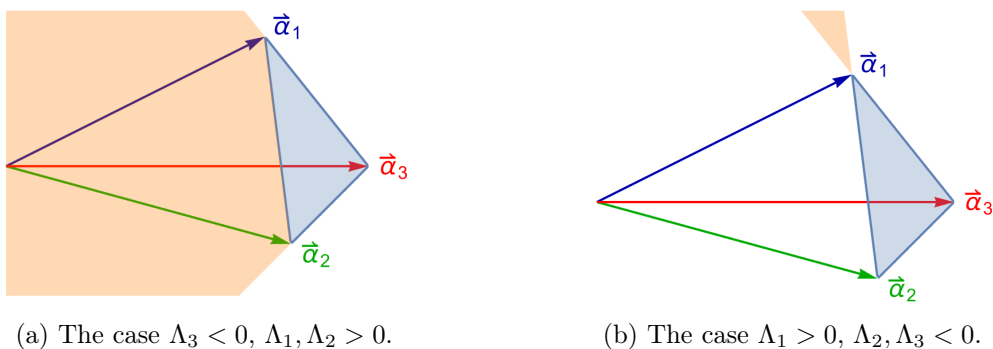


Figure 12: Allowed region of motion for $\vec{\gamma}$, for a three-exponential potential. The blue shaded region is the convex hull of the exponents; it corresponds to the allowed region for the case $\Lambda_i > 0$ for $i = 1, 2, 3$. The allowed region in the case $\Lambda_3 < 0, \Lambda_1, \Lambda_2 > 0$ ($\Lambda_1 > 0, \Lambda_2, \Lambda_3 < 0$) corresponds to the brown shaded region of Figure 12a (Figure 12b).

7 Conclusions

We have studied in detail the universal cosmology models of [16], from the general standpoint of a 4d gravitational theory with two minimally coupled scalars, focusing on the case of negative 3d spatial curvature. We have employed a set of phase space variables that allow for an intuitive interpretation of motion in phase space, and a particularly simple description of the attractor critical point — responsible for the late time properties of the cosmological evolution — in terms of the convex hull of the exponents of the potential.

Our analysis of critical points and stability is in agreement with the literature, whenever they overlap. In particular we find that the stability of critical points of the potential for which both exponentials contribute at late times, cf. Table 6, requires both terms to be positive, as recently emphasized in [43] in the case of flat cosmologies, in agreement with the analysis in [56]. Furthermore, stable points with one positive and one negative exponential are also possible, cf. Table 7, provided the potential is dominated by the positive exponential asymptotically. Such critical points were called *nonproper* in [56], as some scalars become infinite at the critical point. It is also straightforward to verify that the universal acceleration bound given in [39, (II.10)] for a flat cosmology, is satisfied.¹⁷

We have seen that, in all but one model, decompactification is avoided, and both higher-order g_s - and α' -corrections are suppressed at late times. Moreover, three of these models exhibit time-evolution driven scale separation at late times. The models that avoid decompactification at late times but do not exhibit scale separation, all have potentials that contain a 6d curvature contribution that remains non-trivial at late times. We have noted that this contribution does not need to dominate at late times for the absence of scale separation to occur, generalizing the observations of [49], in line with the results of [39] for flat universe. Furthermore we have discussed some mechanisms by which it might be possible to achieve relative (as opposed to parametric) scale separation in these models.

As a side note, we have constructed the fully analytic expression of the eternally accelerating cosmology of [61]. As was noted in [16], this cosmology can be geodesically completed in the past, and has no Big Bang singularity: in the vicinity of the apparent singularity, the space becomes de Sitter in hyperbolic slicing.

As a general rule, the presence of multiple positive exponential terms leads to the lowering of the effective exponent of the potential near the stable critical point. The smallest value of the effective exponent is attained for the model of [16] coming from compactification on an Einstein space with negative curvature and non-vanishing Romans mass, and is smaller than the threshold below which the attractor point P_1 is a stable node (but above the swampland bound). Multiple exponentials thus provide a mechanism that allows to lower the curvature energy density near the critical point, potentially improving the compatibility of these models with observation.

¹⁷The acceleration bound given in [39, (II.10)] is saturated by the stable critical point P_2 of Table 6: in this case our $\gamma_* = \gamma_{ch}$ coincides with $\hat{\gamma}_\infty$ of that reference. Moreover, the bound is also saturated for the critical point P_1 of Table 6, which corresponds to an open cosmology. On the other hand, for the case of one positive and one negative exponential, [39, (II.10)] provides only a lower bound. Indeed $\hat{\gamma}_\infty$ of Figs. 9, 10 and 11 of [39] corresponds to an unstable $\tilde{\gamma}_*$, as in our Figs. 8a and 7b respectively.

Our analysis has mostly focused on two-exponential potentials, which is the case that captures all the essential physics at late times. Although we do not expect the multi-exponential case to alter the physics asymptotically, it is a different story when it comes to detailed universe histories in the bulk of phase space. Indeed the latter would become important if one wishes to generalize the present analysis to a multi-exponential quintessence scenario with the inclusion of a general barotropic fluid, with the aim of modeling radiation and matter throughout the history of the universe — as was done in [45] for the case of a single exponential.

Acknowledgment

We would like to thank George Tringas for collaboration on inflationary aspects of the models considered here, and David Andriot for useful discussions on cosmological scale separation.

References

- [1] P. K. Townsend and M. N. Wohlfarth, *Accelerating cosmologies from compactification*, *Phys. Rev. Lett.* **91** (2003) 061302, [[hep-th/0303097](#)].
- [2] G. Gibbons, *Aspects of supergravity theories*, *GIFT Seminar 1984:0123 (QCD161:G2:1984)* (1984).
- [3] G. Gibbons, *Thoughts on tachyon cosmology*, *Class. Quant. Grav.* **20** (2003) S321–S346, [[hep-th/0301117](#)].
- [4] J. M. Maldacena and C. Nunez, *Supergravity description of field theories on curved manifolds and a no go theorem*, *Int.J.Mod.Phys.* **A16** (2001) 822–855, [[hep-th/0007018](#)].
- [5] J. Russo and P. Townsend, *Late-time Cosmic Acceleration from Compactification*, *Class. Quant. Grav.* **36** (2019), no. 9 095008, [[arXiv:1811.03660](#)].
- [6] J. Russo and P. Townsend, *Time-dependent compactification to de Sitter space: a no-go theorem*, *JHEP* **06** (2019) 097, [[arXiv:1904.11967](#)].
- [7] N. Ohta, *Accelerating cosmologies from S-branes*, *Phys. Rev. Lett.* **91** (2003) 061303, [[hep-th/0303238](#)].
- [8] N. Ohta, *A Study of accelerating cosmologies from superstring / M theories*, *Prog. Theor. Phys.* **110** (2003) 269–283, [[hep-th/0304172](#)].
- [9] N. Ohta, *Accelerating cosmologies and inflation from M/superstring theories*, *Int. J. Mod. Phys. A* **20** (2005) 1–40, [[hep-th/0411230](#)].
- [10] S. Roy, *Accelerating cosmologies from M / string theory compactifications*, *Phys. Lett. B* **567** (2003) 322–329, [[hep-th/0304084](#)].
- [11] M. Gutperle, R. Kallosh, and A. D. Linde, *M / string theory, S-branes and accelerating universe*, *JCAP* **07** (2003) 001, [[hep-th/0304225](#)].
- [12] R. Emparan and J. Garriga, *A Note on accelerating cosmologies from compactifications and S branes*, *JHEP* **05** (2003) 028, [[hep-th/0304124](#)].

- [13] P. K. Townsend, *Cosmic acceleration and M theory*, in *14th International Congress on Mathematical Physics*, pp. 655–662, 8, 2003. [hep-th/0308149](#).
- [14] C.-M. Chen, P.-M. Ho, I. P. Neupane, N. Ohta, and J. E. Wang, *Hyperbolic space cosmologies*, *JHEP* **10** (2003) 058, [[hep-th/0306291](#)].
- [15] M. N. Wohlfarth, *Inflationary cosmologies from compactification?*, *Phys. Rev. D* **69** (2004) 066002, [[hep-th/0307179](#)].
- [16] P. Marconnet and D. Tsimpis, *Universal accelerating cosmologies from 10d supergravity*, *JHEP* **01** (2023) 033, [[arXiv:2210.10813](#)].
- [17] G. D’Amico and N. Kaloper, *Rollercoaster cosmology*, *JCAP* **08** (2021), 058 [[arXiv:2011.09489](#)].
- [18] B. Freivogel, M. Kleban, M. Rodriguez Martinez, and L. Susskind, *Observational consequences of a landscape*, *JHEP* **03** (2006) 039, [[hep-th/0505232](#)].
- [19] A. Bedroya, H. Lee and P. Steinhardt, *A species scale-driven breakdown of effective field theory in time-dependent string backgrounds*, [2504.13260](#).
- [20] D. Andriot, D. Tsimpis, and T. Wrase, *Accelerated expansion of an open universe, and string theory realizations*, *Phys. Rev. D* **108** (2023) no.12, 123515, [[arXiv:2309.03938](#)].
- [21] G. Obied, H. Ooguri, L. Spodyneiko, and C. Vafa, *De Sitter Space and the Swampland*, [arXiv:1806.08362](#).
- [22] A. Hebecker and T. Wrase, *The Asymptotic dS Swampland Conjecture - a Simplified Derivation and a Potential Loophole*, *Fortsch. Phys.* **67** (2019), no. 1-2 1800097, [[arXiv:1810.08182](#)].
- [23] D. Andriot, *Open problems on classical de Sitter solutions*, *Fortsch. Phys.* **67** (2019), no. 7 1900026, [[arXiv:1902.10093](#)].
- [24] D. Lüst, E. Palti, and C. Vafa, *AdS and the Swampland*, *Phys. Lett. B* **797** (2019) 134867, [[arXiv:1906.05225](#)].
- [25] A. Bedroya and C. Vafa, *Trans-Planckian Censorship and the Swampland*, *JHEP* **09** (2020) 123, [[arXiv:1909.11063](#)].
- [26] D. Andriot, N. Cribiori, and D. Erkiner, *The web of swampland conjectures and the TCC bound*, *JHEP* **07** (2020) 162, [[arXiv:2004.00030](#)].
- [27] T. Rudelius, *Dimensional reduction and (Anti) de Sitter bounds*, *JHEP* **08** (2021) 041, [[arXiv:2101.11617](#)].
- [28] T. Rudelius, *Asymptotic observables and the swampland*, *Phys. Rev. D* **104** (2021), no. 12 126023, [[arXiv:2106.09026](#)].
- [29] L. J. Boya, M. A. Per, and A. J. Segui, *Graphical and kinematical approach to cosmological horizons*, *Phys. Rev. D* **66** (2002) 064009, [[gr-qc/0203074](#)].
- [30] P. Agrawal, G. Obied, P. J. Steinhardt, and C. Vafa, *On the Cosmological Implications of the String Swampland*, *Phys. Lett. B* **784** (2018) 271–276, [[arXiv:1806.09718](#)].
- [31] Y. Olguin-Trejo, S. L. Parameswaran, G. Tasinato, and I. Zavala, *Runaway Quintessence, Out of the Swampland*, *JCAP* **01** (2019) 031, [[arXiv:1810.08634](#)].
- [32] A. Hebecker, T. Skrzypek, and M. Wittner, *The F-term Problem and other Challenges of Stringy Quintessence*, *JHEP* **11** (2019) 134, [[arXiv:1909.08625](#)].

- [33] M. Cicoli, G. Dibitetto, and F. G. Pedro, *New accelerating solutions in late-time cosmology*, *Phys. Rev. D* **101** (2020), no. 10 103524, [[arXiv:2002.02695](#)].
- [34] B. Valeixo Bento, D. Chakraborty, S. L. Parameswaran, and I. Zavala, *Dark Energy in String Theory*, *PoS CORFU2019* (2020) 123, [[arXiv:2005.10168](#)].
- [35] M. Cicoli, F. Cunillera, A. Padilla, and F. G. Pedro, *Quintessence and the Swampland: The Parametrically Controlled Regime of Moduli Space*, *Fortsch. Phys.* **70** (2022), no. 4 2200009, [[arXiv:2112.10779](#)].
- [36] T. Rudelius, *Asymptotic scalar field cosmology in string theory*, *JHEP* **10** (2022) 018, [[arXiv:2208.08989](#)].
- [37] J. Calderón-Infante, I. Ruiz, and I. Valenzuela, *Asymptotic accelerated expansion in string theory and the Swampland*, *JHEP* **06** (2023) 129, [[arXiv:2209.11821](#)].
- [38] G. Shiu, F. Tonioni, and H. V. Tran, *Accelerating universe at the end of time*, *Phys. Rev. D* **108** (2023), no. 6 063527, [[arXiv:2303.03418](#)].
- [39] G. Shiu, F. Tonioni, and H. V. Tran, *Late-time attractors and cosmic acceleration*, *Phys. Rev. D* **108** (2023), no. 6 063528, [[arXiv:2306.07327](#)].
- [40] S. Cremonini, E. Gonzalo, M. Rajaguru, Y. Tang, and T. Wrase, *On asymptotic dark energy in string theory*, *JHEP* **09** (2023) 075, [[arXiv:2306.15714](#)].
- [41] A. Hebecker, S. Schreyer, and V. Venken, *No asymptotic acceleration without higher-dimensional de Sitter vacua*, *JHEP* **11** (2023) 173, [[arXiv:2306.17213](#)].
- [42] J. Freigang, D. Lust, G.-E. Nian, and M. Scalisi, *Cosmic acceleration and turns in the Swampland*, *JCAP* **11** (2023) 080, [[arXiv:2306.17217](#)].
- [43] T. Van Riet, *No accelerating scaling cosmologies at string tree level?*, *JCAP* **01** (2024) 055, [[arXiv:2308.15035](#)].
- [44] G. Shiu, F. Tonioni, and H. V. Tran, *Collapsing universe before time*, *JCAP* **05** (2024) 124, [[arXiv:2312.06772](#)].
- [45] D. Andriot, S. Parameswaran, D. Tsimpis, T. Wrase, and I. Zavala, *Exponential quintessence: curved, steep and stringy?*, *JHEP* **08** (2024) 117, [[arXiv:2405.09323](#)].
- [46] G. Shiu, F. Tonioni, and H. V. Tran, *Analytic bounds on late-time axion-scalar cosmologies*, *JHEP* **09** (2024) 158, [[arXiv:2406.17030](#)].
- [47] G. F. Casas and I. Ruiz, *Cosmology of light towers and swampland constraints*, *JHEP* **12** (2024) 193, [[arXiv:2409.08317](#)].
- [48] D. Andriot, *Quintessence: an analytical study, with theoretical and observational applications*, [[arXiv:2410.17182](#)].
- [49] D. Andriot, N. Cribiori, and T. Van Riet, *Scale separation, rolling solutions and entropy bounds*, [[arXiv:2504.08634](#)].
- [50] **DESI** Collaboration, M. Abdul Karim et al., *DESI DR2 Results II: Measurements of Baryon Acoustic Oscillations and Cosmological Constraints*, [[arXiv:2503.14738](#)].
- [51] **DESI** Collaboration, K. Lodha et al., *Extended Dark Energy analysis using DESI DR2 BAO measurements*, [[arXiv:2503.14743](#)].
- [52] S. Bhattacharya, G. Borghetto, A. Malhotra, S. Parameswaran, G. Tasinato, and I. Zavala, *Cosmological constraints on curved quintessence*, *JCAP* **09** (2024) 073, [[arXiv:2405.17396](#)].

- [53] G. Alestas, M. Delgado, I. Ruiz, Y. Akrami, M. Montero, and S. Nesseris, *Is curvature-assisted quintessence observationally viable?*, *Phys. Rev. D* **110** (2024), no. 10 106010, [[arXiv:2406.09212](#)].
- [54] Y. Akrami, G. Alestas and S. Nesseris, *Has DESI detected exponential quintessence?*, [2504.04226](#).
- [55] E. J. Copeland, A. R. Liddle, and D. Wands, *Exponential potentials and cosmological scaling solutions*, *Phys. Rev. D* **57** (1998) 4686–4690, [[gr-qc/9711068](#)].
- [56] J. Hartong, A. Ploegh, T. Van Riet, and D. B. Westra, *Dynamics of generalized assisted inflation*, *Class. Quant. Grav.* **23** (2006) 4593–4614, [[gr-qc/0602077](#)].
- [57] J. Halliwell, *Scalar Fields in Cosmology with an Exponential Potential*, *Phys. Lett. B* **185** (1987) 341.
- [58] R. J. van den Hoogen, A. A. Coley, and D. Wands, *Scaling solutions in Robertson-Walker space-times*, *Class. Quant. Grav.* **16** (1999) 1843–1851, [[gr-qc/9901014](#)].
- [59] Z.-K. Guo, Y.-S. Piao, R.-G. Cai, and Y.-Z. Zhang, *Cosmological scaling solutions and cross coupling exponential potential*, *Phys. Lett. B* **576** (2003) 12–17, [[hep-th/0306245](#)].
- [60] R. J. van den Hoogen and L. Filion, *Stability analysis of multiple scalar field cosmologies with matter*, *Class. Quant. Grav.* **17** (2000) 1815–1825.
- [61] L. Andersson and J. Heinzle, *Eternal acceleration from M-theory*, *Adv. Theor. Math. Phys.* **11** (2007), no. 3 371–398, [[hep-th/0602102](#)].
- [62] T. Barreiro, E. J. Copeland, and N. J. Nunes, *Quintessence arising from exponential potentials*, *Phys. Rev. D* **61** (2000) 127301, [[astro-ph/9910214](#)].
- [63] X.-Z. Li, Y.-B. Zhao, and C.-B. Sun, *Heteroclinic orbit and tracking attractor in cosmological model with a double exponential potential*, *Class. Quant. Grav.* **22** (2005) 3759–3766, [[astro-ph/0508019](#)].
- [64] L. Jarv, T. Mohaupt and F. Saueressig, *Quintessence cosmologies with a double exponential potential*, *JCAP* **08** (2004), 016, [[hep-th/0403063](#)].
- [65] A. R. Liddle, A. Mazumdar, and F. E. Schunck, *Assisted inflation*, *Phys. Rev. D* **58** (1998) 061301, [[astro-ph/9804177](#)].
- [66] A. A. Coley and R. J. van den Hoogen, *The Dynamics of multiscalar field cosmological models and assisted inflation*, *Phys. Rev. D* **62** (2000) 023517, [[gr-qc/9911075](#)].
- [67] E. J. Copeland, A. Mazumdar, and N. J. Nunes, *Generalized assisted inflation*, *Phys. Rev. D* **60** (1999) 083506, [[astro-ph/9904309](#)].
- [68] A. Collinucci, M. Nielsen, and T. Van Riet, *Scalar cosmology with multi-exponential potentials*, *Class. Quant. Grav.* **22** (2005) 1269–1288, [[hep-th/0407047](#)].
- [69] P. J. Steinhardt, L.-M. Wang, and I. Zlatev, *Cosmological tracking solutions*, *Phys. Rev. D* **59** (1999) 123504, [[astro-ph/9812313](#)].
- [70] J. Wainwright and G. F. R. Ellis, *Dynamical systems in cosmology*. Cambridge University Press, 1997.
- [71] S. Bahamonde, C. G. Böhm, S. Carloni, E. J. Copeland, W. Fang, and N. Tamanini, *Dynamical systems applied to cosmology: dark energy and modified gravity*, *Phys. Rept.* **775-777** (2018) 1–122, [[arXiv:1712.03107](#)].

- [72] D. Tsimpis, *Supersymmetric AdS vacua and separation of scales*, *JHEP* **08** (2012) 142, [[arXiv:1206.5900](#)].
- [73] J.-M. Richard, R. Terrisse, and D. Tsimpis, *On the spin-2 Kaluza-Klein spectrum of $AdS_4 \times S^2(\mathcal{B}_4)$* , *JHEP* **12** (2014) 144, [[arXiv:1410.4669](#)].
- [74] F. Marchesano, E. Palti, J. Quirant, and A. Tomasiello, *On supersymmetric AdS_4 orientifold vacua*, *JHEP* **08** (2020) 087, [[arXiv:2003.13578](#)].
- [75] F. F. Gautason, M. Schillo, T. Van Riet, and M. Williams, *Remarks on scale separation in flux vacua*, *JHEP* **03** (2016) 061, [[arXiv:1512.00457](#)].
- [76] A. Font, A. Herráez, and L. E. Ibáñez, *On scale separation in type II AdS flux vacua*, *JHEP* **03** (2020) 013, [[arXiv:1912.03317](#)].
- [77] D. Lüst and D. Tsimpis, *AdS_2 type-IIA solutions and scale separation*, *JHEP* **07** (2020) 060, [[arXiv:2004.07582](#)].
- [78] D. Junghans, *O-Plane Backreaction and Scale Separation in Type IIA Flux Vacua*, *Fortsch. Phys.* **68** (2020), no. 6 2000040, [[arXiv:2003.06274](#)].
- [79] F. Farakos, G. Tringas, and T. Van Riet, *No-scale and scale-separated flux vacua from IIA on G_2 orientifolds*, *Eur. Phys. J. C* **80** (2020), no. 7 659, [[arXiv:2005.05246](#)].
- [80] G. B. De Luca and A. Tomasiello, *Leaps and bounds towards scale separation*, *JHEP* **12** (2021) 086, [[arXiv:2104.12773](#)].
- [81] N. Cribiori, D. Junghans, V. Van Hemelryck, T. Van Riet, and T. Wrase, *Scale-separated AdS_4 vacua of IIA orientifolds and M-theory*, *Phys. Rev. D* **104** (2021), no. 12 126014, [[arXiv:2107.00019](#)].
- [82] D. Tsimpis, *Relative scale separation in orbifolds of S^2 and S^5* , *JHEP* **03** (2022) 169, [[arXiv:2201.10916](#)].
- [83] F. Apers, M. Montero, T. Van Riet, and T. Wrase, *Comments on classical AdS flux vacua with scale separation*, *JHEP* **05** (2022) 167, [[arXiv:2202.00682](#)].
- [84] F. Farakos and M. Moritsu, *Scale-separated $AdS_3 \times S^1$ vacua from IIA orientifolds*, *Eur. Phys. J. C* **84** (2024), no. 1 98, [[arXiv:2311.08991](#)].
- [85] T. Coudarchet, *Hiding the extra dimensions: A review on scale separation in string theory*, *Phys. Rept.* **1064** (2024) 1–28, [[arXiv:2311.12105](#)].
- [86] A. Arboleya, A. Guarino, and M. Moritsu, *Type II orientifold flux vacua in 3D*, *JHEP* **12** (2024) 087, [[arXiv:2408.01403](#)].
- [87] N. Cribiori, F. Farakos, and N. Liatsos, *On scale-separated supersymmetric AdS_2 flux vacua*, *Eur. Phys. J. C* **85** (2025), no. 2 213, [[arXiv:2411.04932](#)].
- [88] V. Van Hemelryck, *Supersymmetric scale-separated AdS_3 vacua of type IIB*, [[arXiv:2502.04791](#)].
- [89] G. Tringas and T. Wrase, *Scale separation from O-planes*, [[arXiv:2504.15436](#)].
- [90] A. Proust, H. Samtleben, and E. Sezgin, *Scale separation on $AdS_3 \times S^3$ with and without supersymmetry*, [[arXiv:2504.12425](#)].
- [91] T. C. Collins, D. Jafferis, C. Vafa, K. Xu, and S.-T. Yau, *On Upper Bounds in Dimension Gaps of CFT's*, [[arXiv:2201.03660](#)].